# Historical climate variability reconstructed from massive coral records in the western Indian Ocean

**Jean Vincent Arnaud Nicolas (UCT)** (ID No: NCLJEA002)

*Supervisor:* **Prof. Chris Reason (UCT)**

*Co-supervisor:* **Dr. Jens Zinke (UWA)**



MSc in Applied Marine Science

Department of Oceanography

**University of Cape Town**

**2012**

**Table of contents**

***Page***

## List of Figures

***Page***

## List of Tables

***Page***

**Abstract**

Coral $\delta^{18}O$ and Sr/Ca records from massive corals in the western Indian Ocean (WIO) are used to establish the heterogeneous distribution of warming rates across the tropical and subtropical regions and to investigate if it corresponds with that from instrumental sea surface temperatures (SSTs). The coral records correlate with instrumental data better on monthly time scales compared to annual time scales. Coral thermal stress was assessed by the Degree Heating Months (DHM) technique and even though the coral DHM aligns quite well with instrumental DHM, the values from coral data are generally 2-3 times greater in magnitude than the DHM values from instrumental data. It was found that the accumulated thermal stress, calculated from coral and instrumental data, for the majority of the tropical and subtropical WIO sites has been increasing since the 1970's. From 1870 to 1995, both the tropics and the subtropics have been warming in general, although with different and varying rates as recorded by the coral and the instrumental SSTs. It was further revealed that both the tropical and the subtropical WIO warmed during the summer and winter periods during 1870-1995. On longer time scales, the relationship between the coral records in the WIO and climate indices showed a significant interannual variability approximately centered at periods 3-6 years, indicating a probable link with ENSO and IOD. The extent to which coral reefs from different sites in the WIO are prepared to survive climate change based on historical SST variability and intensity of warming rates are described. It could therefore be suggested that some corals may be more favoured to survive warming climate compared to others because corals in the WIO are located in different oceanographic conditions and experience different climatic variations.

**Keywords**: coral records; $\delta^{18}O$; Sr/Ca; corals; western Indian Ocean (WIO); warming rate; sea surface temperatures (SSTs); Degree Heating Months (DHM); climate change

# 1.0. Introduction

## 1.1. Geochemical proxies from corals

Paleoclimate data have been obtained from massive corals during the last few decades (Gagan et al., 2000; Zinke et al., 2009) in the tropical and subtropical regions across the globe. Information about the temperature and composition of the seawater in which corals live are recorded in the chemistry and configuration of their skeletons as they grow (Cobb et al., 2008). Coral skeletons provide very good natural records of past environmental conditions (Eakin and Grottoli, 2006) and variability in past climates can be deduced on interannual to multidecadal timescales by analysing the geochemical parameters in the skeletons of living coral colonies (Charles et al., 2003, Cole et al., 1993, 2000; Gagan et al., 1998; Pfeiffer et al., 2004a, b , 2006; Zinke et al., 2005, 2009).

The geochemical tracers in the aragonite skeletons of reef-building corals such as *Porites* spp., are mostly used to infer past values of sea surface temperature (SST) (Eakin and Grottoli, 2006). However, other proxy records from corals such as $\delta^{18}O$, Mn/Ca, Cd/Ca and Ba/Ca are used to reconstruct past sea surface salinity (SSS), winds and upwelling, river runoff, pollutants and ocean mixing (Eakin and Grottoli, 2006). The $\delta^{18}O$, Sr/Ca, U/Ca, Mg/Ca records in corals can be used as proxies for reconstruction of past SST. Since massive corals living in association with symbiotic microalgae are found in the photic zone of the tropical and subtropical oceans at around 1-20 m deep, the proxy signatures in their skeletons will record the conditions prevailing in the upper ocean surface in coral reef ecosystems. Gagan et al. (2000) and Corrège (2006) reported that $\delta^{18}O$ and Sr/Ca coral records are the most reliable paleotemperature proxies.

$\delta^{18}O$ is the ratio of $^{18}O$ to $^{16}O$ and it is a function of both SST and $\delta^{18}O$ of the ambient seawater ($\delta^{18}O_{seawater}$) (Cole et al., 1993). The $\delta^{18}O_{seawater}$ is influenced by the balance between evaporation and precipitation of a particular region (Juillet-Leclerc et al., 1997). Rainfall, evaporation, advection of water masses, and freshwater runoff can all affect $\delta^{18}O_{seawater}$ as described by Lough (2010). In regions where $\delta^{18}O$ is constant, coral $\delta^{18}O$ gives variations in SST, and in regions where the balance between evaporation and precipitation varies, coral $\delta^{18}O$ generally records sea surface salinity (SSS), rainfall or freshwater runoff (Lough, 2010). A rise in temperature leads to a decrease in the $^{18}O$ fractionation of the coral skeleton (Kim and O'Neil, 1997), implying that corals will incorporate more of the lighter $^{16}O$ in their skeletons with a rise in SST. Therefore, $\delta^{18}O$ signal in corals will decrease with higher temperature.

The Sr/Ca ratio is more or less a direct proxy for temperature since it is not influenced by salinity (Eakin and Grottoli, 2006). Improvements in analytical techniques, notably by the use of thermal

ionisation mass spectrometry (TIMS), have led to the increased application of Sr/Ca ratios in coral skeletons as a coral proxy for temperature (Beck et al., 1992). Beck et al. (1992) reported that Sr is replaced by Ca in the coral aragonite skeleton by heat exchange processes and less Ca is replaced by heavier divalent cations when temperature increases. The Sr/Ca ratio in coral skeletons decreases with higher temperature.

### 1.2. Coral records, El Niño-Southern Oscillation (ENSO), Indian Ocean Dipole (IOD) and Pacific Decadal Oscillation (PDO)

Owing to insufficient long-term instrumental and observational data in the tropical and subtropical regions, much importance has been given to coral paleoclimatic data in order to analyse past climates prior to the instrumental period. Various studies dealing with coral paleoclimate have been performed in the tropical Pacific owing to the significance of El Niño-Southern Oscillation (ENSO) in global climate variability (Gagan et al., 2000). Scott et al. (2010) described ENSO as one of the major interannual modes of climate variability that has impacts across the globe, with pronounced tropical SST signatures in the Pacific Ocean. The natural match-up of corals as a source of proxy data with ENSO variability before the instrumental era has been possible due to the fact that the location of corals and the origin of ENSO both lie within the tropical Pacific (Eakin and Grottoli, 2006).

Corrège (2006) found that a generally good correlation was observed between the central Pacific and the Indian Ocean including the Red Sea, when analysing high resolution and continuous $\delta^{18}O$ and Sr/Ca coral records from these regions. This result may imply that teleconnections between the oceans are possibly being affected by global warming (Corrège, 2006). Based on coral $\delta^{18}O$ records from the tropical and subtropical western Indian Ocean (WIO), Zinke et al. (2005) found that there are evident teleconnections between the WIO and ENSO in the proxy data, consistent with analysis of instrumental data (e.g. Reason et al., 2000).

The Indian Ocean Dipole (IOD) which is a coupled ocean-atmosphere phenomenon occurring in the equatorial Indian Ocean is considered as one major mode of interannual SST variability (Saji et al. 1999; Hong et al., 2008). The IOD occurs independently of the ENSO in the Pacific Ocean (Saji et al. 1999) and it has been recently revealed that IOD can be recognized without ENSO signals (Cai et al., 2005). A positive IOD occurs when the water in the tropical western Indian Ocean is abnormally warmer compared to the tropical eastern Indian Ocean which experienced cooler than normal water (Saji et al. 1999). On the other hand, a negative IOD is characterised by cooler than normal water in the tropical western Indian Ocean while anomalously warmer water is recorded in the tropical

eastern Indian Ocean (Saji et al. 1999). IOD events can occur with or without ENSO and there are years where both phenomena do coincide (Hong et al., 2008). During the last 3 centuries, the variability of ENSO and IOD in the WIO have been identified in coral proxy records (Charles et al., 1997; Cole et al., 2000; Zinke et al., 2004, 2005).

ENSO years include 1972-1973, 1982-1983, 1987-1988, 1991-1992, 1997-1998 (Saji et al., 1999). In the earlier period, major ENSO events occurred in 1789-1793, 1828, 1876-1878, 1891, 1925-1926, 1941-1942 and 1957-1958 (National Climatic Data Centre, 2009) and in the most recent time ENSO took place in 2002-2003, 2004-2005, 2006-2007 and 2009. As for the positive IOD events, they occurred in 1961, 1963, 1966-1967, 1972, 1976-1977, 1982-1983, 1987, 1994 and 1997 and years where positive IOD-ENSO events coincide are 1963, 1972, 1976, 1982, 1987, 1997 (Hong et al., 2008) and 1983 and 1988 are also included as positive IOD-ENSO years in this study. Meyers et al. (2007) gave a classification of the years when El Niño or La Niña and/or positive or negative IOD took place from 1877 to 1998, while Ummenhofer et al. (2009) made improvements and updated the classification up to the year 2008.

The most dominant interannual climate variability is linked to ENSO. However, the trend of its teleconnection is controlled by climate variability on interdecadal variability, notably the Pacific Decadal Oscillation (PDO) (Mantua and Hare, 2002). The PDO modulates the ENSO signal in the Pacific Ocean and remotely in the Indian Ocean (Mantua and Hare, 2002; Crueger et al., 2009). In fact, the PDO fingerprint is not well recorded by the short instrumental data since it is a low-frequency phenomenon. A link does exists between the PDO and climate variability on decadal time scales in the south-western Indian Ocean (Allan et al., 1995; Deser et al., 2004; Reason and Rouault, 2002). To overcome the short and insufficient long-term instrumental data to detect the PDO signals, coral proxy data could used in this respect (e.g Linsley et al., 2004). Pfeiffer et al. (2004b) attempted to detect PDO fingerprint in corals from Reunion Island and Crueger et al. (2009) revealed that PDO signals were captured from coral $\delta^{18}O$ data from two locations in the WIO.

Coral proxies have not only helped in reconstructing modern climate but have also been used to infer past climatic conditions prevailing during the Holocene, the Last Glacial Maximum and the last Interglacial (Eakin and Grottoli, 2006). Rather than being used directly to reconstruct temperatures, geochemical proxies from massive corals are mostly used as relative indicators of temperatures mainly due to concerns regarding calibration (Eakin and Grottoli, 2006). Calibration with different degrees of precision have been done by comparing geochemical proxies from living coral colonies with temperatures obtained from both *in-situ* and satellite measurements (Eakin and Grottoli, 2006).

### 1.3. SST data from in situ instruments and satellite

SST data derived from ship of opportunity measurements collected in the International Comprehensive Ocean-Atmosphere Data Set (ICOADS) were used to analyse the trends in warming since the 1850s and to calibrate coral SST proxies (Scott et al., 2010). However, it is important to highlight the fact that instrumental data does have limitations (Scott et al., 2010). The Hadley Centre SST dataset version 1.1 (HadSST1.1) (Rayner et al., 2003) and the NOAA Extended Reconstructed SST dataset version 3 (ERSSTv3) (Smith et al., 2008a) are used in this study and are examples of instrumental SST data mostly obtained from ships and buoys measurements. HadSST1.1 is a monthly global field of SST averaged on 1° latitude by 1° longitude regular grid from 1870 to present. Horizontal interpolation was applied to fill in gaps in the HadSST1.1 dataset. ERSSTv3 is a monthly-mean SST on a 2°x2° regular grid from 1854. There are no missing data since the gaps have been filled by using an EOF-based reconstruction technique (Smith et al., 2008a).

Concerning satellite SST data, the Advanced Very High Resolution Radiometer (AVHRR) SST (Reynolds et al., 2007) is the most appropriate to use and has the advantage over HadSST1.1 and ERSSTv3 data of a finer resolution grid. In fact, SST data from AVHRR sensor has a resolution of 0.25° in space and a temporal resolution of 1 day. However, cloud coverage and its short duration (available from 1981) are the major limitations of AVHRR SST.

### 1.4. Coral thermal stress and coral bleaching

During El Niño and positive Indian Ocean Dipole (IOD) events in the WIO, positive SST anomalies are frequently recorded across the tropics and subtropics, and a $1^{o}$ C increase above the monthly mean maximum often causes coral bleaching (Strong et al., 1997). Coral bleaching refers to the loss of microalgae that live in symbiosis with the coral polyps and/or a decline in photosynthetic pigment concentrations in the symbiotic microlagae from corals, mainly due to thermal stress (Hoegh-Guldberg, 1999). Two techniques based on SSTs obtained from satellites have been employed to measure coral thermal stress (Strong et al., 1997). They are firstly, a high temperature “threshold” technique (Goreau and Hayes, 1994) or a bleaching index based on “degree heating weeks” (DHW), and secondly, a “hot spots” technique which is described as regions of abnormally high SSTs going beyond $+1^{o}$ C above the warmest monthly mean SST, based on climatology (Strong et al., 1997). Similarly to DHW, Lough (2000) used “degree heating months” (DHM) to assess the long-term trends of coral thermal stress. The DHM is normally calculated by adding the monthly temperature anomalies which are greater than the long-term mean maximum monthly temperature (Carilli et al.,

2010). Coral bleaching in the WIO has been well forecasted by the DHM measure (McClanahan et al., 2007).

### 1.5. The WIO and coral records

McClanahan et al. (2011) described the WIO as a biogeographic section of the Indian Ocean that stretches from the shores of East Africa to the banks of the Mascarene Plateau. Spalding et al. (2001) reported that the WIO has a rich biodiversity comprising mostly of coral reefs that occupy about 7000km$^2$. Long *Porites spp.* coral data records for the WIO region are available for download at the NOAA Paleoclimate Data base website, as shown in Table 1.1. Coral records are available both from the tropical and subtropical WIO regions, with the 10$^o$ latitude line being the dividing line between these two regions. Table 1.2. shows the sites, core names and locations from which coral proxy data were obtained and used in this study. Figure 1.1. shows a map of the study area and the locations where the coral cores used in this study were taken. The tropical sites include Seychelles, Chagos Archipelago, Kenya, Tanzania and the subtropical sites comprise of Mayotte (Comoro Archipelago), Madagascar, Reunion Island and Rodrigues Island. In general, SST data from *in-situ* instruments and satellite are limited and in short supply in the WIO (Zinke et al., 2005). By contrast, coral records from the WIO have successfully provided monthly to annual datasets of SST, SSS and precipitation for more than 3 centuries (Charles et al., 2003, Cole et al., 2000, Zinke et al., 2004a, b, 2005; Pfeiffer et al., 2004a, b).

It is important to assess how well coral records correlate with regional scale SST variability, particularly in determining the slope of calibration of coral SST proxies. Most authors that analysed coral records from the WIO compared the coral $\delta^{18}O$ records with ERSST (Smith and Reynolds, 2003). Zinke et al. (2009) computed the correlation measurements between coral $\delta^{18}O$ records with ERSST (Smith and Reynolds, 2003) performed by previous workers (Pfeiffer and Dullo, 2006; Charles at al., 1997; Cole et al., 2000; Zinke et al., 2005; Zinke et al., 2004a, b; Pfeiffer et al., 2004b) in the WIO and found that all coral $\delta^{18}O$ records correlate significantly with regional SST variability, except that from Reunion Island as discussed by Pfeiffer et al. (2004b). Scott et al. (2010) summarised the correlation studies done by some authors between Sr/Ca and AVHRR SST and concluded that there is significant correlation between the coral proxy and instrumental SST in question, but strongest correlation was observed for the seasonal cycle as compared to longer time period such as on annual time scales.

Based on these analyses, this study will establish the heterogeneous distribution of warming rates across the WIO from coral proxy records and to observe if it corresponds with that from

instrumental data or if higher/lower warmings rates are observed for certain regions. In fact, changes in warming rates and variability in SST may have potential impacts on the survival rates of coral reefs in the WIO in respect to future warming.

**Table 1.1. Site, period of coral records, the tracers and the contributors for the WIO region. (Source: NOAA Paleoclimate Data base website)**

| | Site | Core name | Period of record | Tracers | Contributors |
|---|---|---|---|---|---|
| Tropical | Seychelles | BVB | 1846-1995 | $\delta^{18}O$ | Charles, C.D., D.E.Hunter, and R.G.Fairbanks. (1997) |
| | Chagos | Chagos | 1961-1995 | $\delta^{18}O$ | Pfeiffer, M., W.-C. Dullo, and A. Eisenhauer. (2004a) |
| | Kenya | Malindi | 1801-1994 | $\delta^{18}O$ | Cole, J. E., R. B. Dunbar, T. R. McClanahan, and N. Muthiga, (2000) |
| | Tanzania | Mafia | 1896-1998 | $\delta^{18}O$ | Damassa, T.D., J.E. Cole, H.R. Barnett, T.R. Ault, and T.R. McClanahan. (2006) |
| Subtropical | Mayotte | Mayotte | 1881-1993 | $\delta^{18}O$ | Zinke, J., M. Pfeiffer, O. Timm, W.-C. Dullo, D. Kroon, and B. A. Thomassin. (2008) |
| | Madagascar | Ifaty | 1659 - 1995 | $\delta^{18}O$ and *(Sr/Ca) **not a continuous record* | Zinke, J., W.-C. Dullo, G.A. Heiss, and A. Eisenhauer. (2004) |
| | Reunion Is. | Reunion | 1832-1995 | $\delta^{18}O$ | Pfeiffer, M., O. Timm, W.-C. Dullo, and S. Podlech. (2004b) |

**Table 1.2. Site, core name, contributors and approximate GPS locations from which the coral proxy data were obtained. (Coral records obtained from the NOAA Paleoclimate Data base website and from Dr. Jens Zinke)**

| | Site | Core name | Contributors | Approx. GPS location | |
|---|---|---|---|---|---|
| | | | | Latitude | Longitude |
| Tropical | Seychelles | BVB | Charles, C.D., D.E.Hunter, and R.G.Fairbanks. (1997) | 4° S | 55°E |
| | | NEP | Pfeiffer, M. and Dullo, W-C. (2006) | | |
| | | MAHE | Pfeiffer, M. and Dullo, W-C. (2006) | | |
| | Chagos | Chagos | Pfeiffer, M., W.-C. Dullo, and A. Eisenhauer. (2004a) | 5° S | 71° E |
| | | GIM | Pfeiffer, M. and Dullo, W-C. (2006) | | |
| | Kenya | Malindi | Cole, J. E., R. B. Dunbar, T. R. McClanahan, and N. Muthiga. (2000) | 3°S | 40°E |
| | Tanzania | Mafia Archipelago | Damassa, T.D., J.E. Cole, H.R. Barnett, T.R. Ault, and T.R. McClanahan. (2006) | 8° S | 39° E |
| Subtropical | Mayotte | Mayotte | Zinke, J., M. Pfeiffer, O. Timm, W.-C. Dullo, D. Kroon, and B. A. Thomassin. (2008) | 12° S | 45°E |
| | Madagascar (north-eastern region) | Big Mum | Zinke, J., and co-workers. (unpublished) | 12° S | 49° E |
| | Madagascar (Antongil Bay, north-eastern region) | MAS1, ANDRA, IFAHO | Zinke, J., and co-workers. (unpublished) | 15°S | 49° E |
| | Madagascar (Ste. Marie Is, north-eastern region ) | STM2, STM4 | Zinke, J., and co-workers. (unpublished) | 17°S | 49° E |
| | Madagascar (south-western region) | Ifaty cores | Zinke, J., W.-C. Dullo, G.A. Heiss, and A. Eisenhauer. (2004) Zinke, J., Pfeiffer, M., | 23°S | 43° E |

**Table 1.2.** ***continued…***

| | | | | | |
|---|---|---|---|---|---|
| | | | Timm, O., Dullo, W.-C. and Brummer, G. J. A. (2009) | | |
| | Reunion Is. | LaRE cores and St. Rose | Zinke, J., Pfeiffer, M., Timm, O., Dullo, W.-C. & Davies, G. R. (2005)<br><br>Zinke, J., Pfeiffer, M., Timm, O., Dullo, W.-C. and Brummer, G. J. A. (2009) | 21°S | 55° E |
| | Rodrigues Is. | Totor and Cabri | Zinke, J., and co-workers. (unpublished) | 19°S | 63° E |

Coral reefs which experience lower warming rates and possess naturally high SST variability might be geared better for survival compared to reefs with high warming rates and low SST variability. Initially, correlation of coral records with satellite SST data in the WIO will be performed. Then, DHM will be calculated from the coral records and from *in-situ* and satellite SST data, followed by the calculation of warming rates in the tropical and subtropical WIO regions. Lastly, wavelet analyses will be performed on the coral data in order to analyse the significance of longer time scale (interannual to interdecadal) variability in the records.

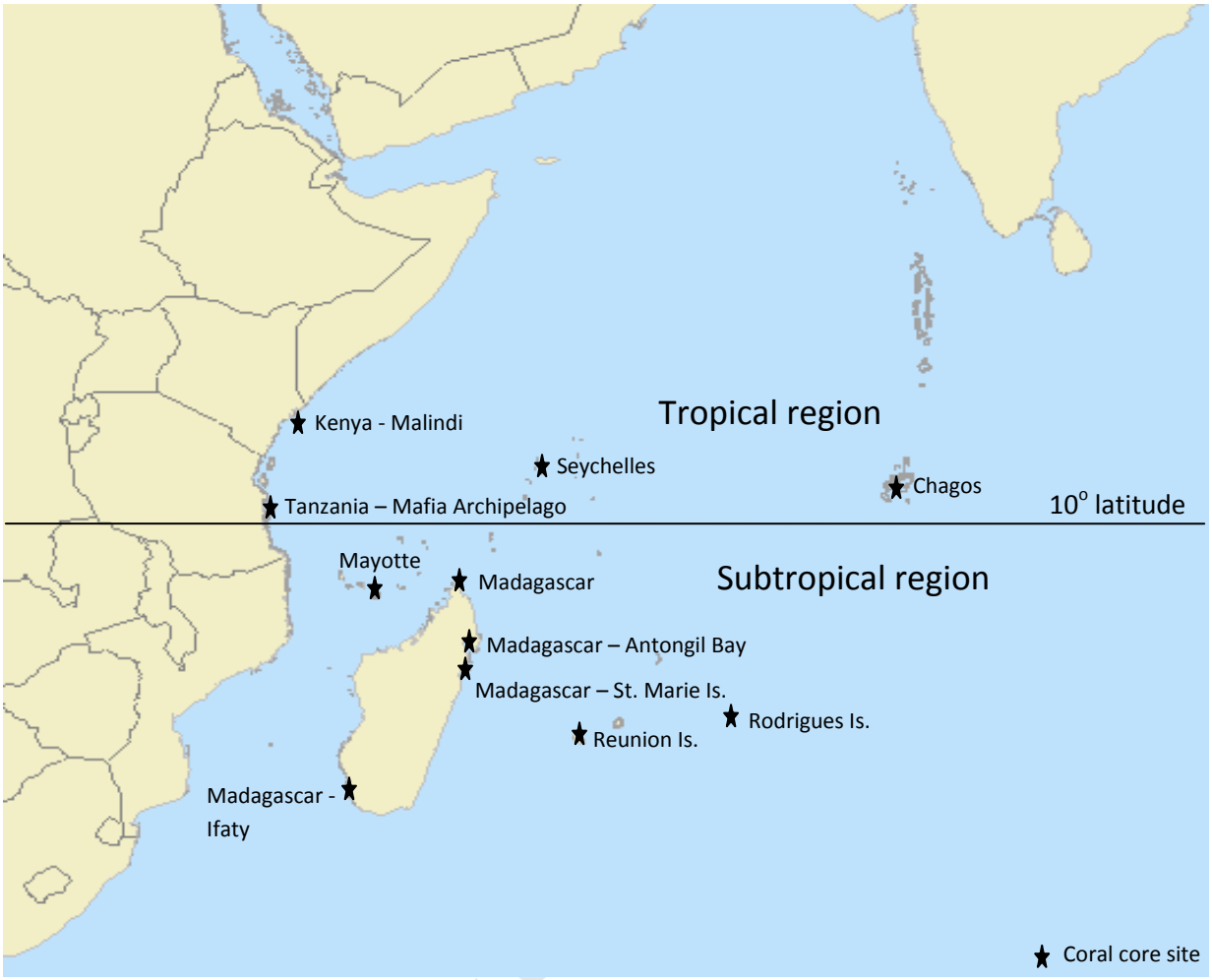


**Figure 1.1. Map of Western Indian Ocean showing coral core sites**. *(Map obtained from: http://reefgis.reefbase.org)*

## 2.0. Methodology

### *2.1. Coral records data*

Coral records data from the tropical and subtropical regions in the WIO (Figure 1.1 and Table 1.1) were downloaded from the NOAA Paleoclimate Data base website, available at *http://www.ncdc.noaa.gov/paleo/corals.html*. Additional coral record data sets were made available by Dr. Jens Zinke. The methods used in coral sampling and coral chronology of the different cores are described in papers from the various contributors, found on the NOAA Paleoclimate Data base website and in Table 1.1 and 1.2. The coral geochemical series from the sampling sites contain either $\delta^{18}O$ or Sr/Ca, but for some sites both tracers are available.

### *2.2. Correlation of coral records with satellite sea surface temperature (SST) data*

Linear correlation (Jaisingh, 2005) is performed between the coral records and AVHRR SST (Reynolds et al., 2007) starting in 1982, since the AVHRR SST data is available as from December 1981 . The AVHRR SST data for each site is found at the same coordinates or interpolated from the nearest grid points, where coral cores were taken. The correlation is done both on monthly and annual time scales. A simple arithmetic mean is computed with the monthly coral records data and the AVHRR SST data in order to obtain the respective annual means. In some cases, like for Chagos and Mayotte, only bimonthly data are available for the coral records and are therefore used for calculation. For each correlation done, the regression equation and the linear correlation coefficient are reported. In order to highlight the uncertainty in the slopes, the confidence intervals are given.



### *2.3. Degree Heating Month*

DHM is calculated from coral proxy data by adding the monthly temperature anomalies greater than the long-term mean maximum monthly temperature, based on climatology (Lough, 2000; Carilli et al., 2010). In climatology, the period 1961-1990 is often used as the reference period to calculate anomalies. To calculate the monthly temperature anomalies, the monthly coral proxy data are firstly centred relative to the mean over the entire datasets. The coral data is then converted into coral SST following the known coral proxy/SST relationship. In order to know the latter relationship, a linear regression between coral proxy and SST at each specific site needs to be done and the slope of regression is reported, similar to what is performed in section 2.2. For Sr/Ca, the formula of the regression equation is: Sr/Ca (mmol/mol)= a+b*SST ($^{o}C$) and for $\delta^{18}O$, it is: $\delta^{18}O$(‰ $^{o}C^{-1}$)= a+b*SST($^{o}C$), where a= y-intercept and b= slope (Corrège, 2006; Juillet-Leclerc, 2001).

For $\delta^{18}O$, the value of the slope of the calibration generally varies between -0.18‰ $^{o}C^{-1}$ and -0.22‰ $^{o}C^{-1}$, and the mean value -0.20 ‰ $^{o}C^{-1}$ is often used in calculations (Corrège, 2006). For Sr/Ca, the slope varies between -0.04 mmol/mol $^{o}C^{-1}$ and -0.08 mmol/mol $^{o}C^{-1}$ with a mean value of -0.06 mmol/mol $^{o}C^{-1}$ which is used in conversions (Juillet-Leclerc, 2001). Finally, the 1961-1990 mean of the centred SST data is calculated and subtracted from the latter to obtain the SST anomalies used for the calculation of DHM. It should be noted that the DHM from coral data has a large uncertainty which is based on the slope uncertainties obtained from the regression of coral data versus SST. The commonly used uncertainty (expressed as ±SE, standard error) for $\delta^{18}O$-SST relationship is ±0.02 ‰ $^{o}C^{-1}$ and for Sr/Ca-SST, it is ±0.02 mmol/mol $^{o}C^{-1}$.

DHM is also calculated from the instrumental data, notably the HadSST1.1 (Rayner et al., 2003) and the ERSSTv3 (Smith et al., 2008a) long-term data sets, in order to assess the thermal stress recorded from instruments and to investigate if the same trend is observed with coral data. The calculation of SST anomalies from the instrumental data is also done relative to the 1961-1990 period. The tropical coral and instrumental data chosen for calculation of DHM are from Seychelles, Chagos, a combination of Seychelles and Chagos records, and in the subtropics the data are from Reunion Island, Rodrigues Island, Madagascar (St. Marie Island, Antongil Bay, north-eastern region and south-western region) and Tanzania (Mafia) records. The Chagos, Seychelles, Rodrigues, Reunion and Madagascar (south-western region) coral records used for this exercise are composites which are calculated by the arithmetic mean of the cores available for any time interval, whereas the Madagascar (St. Marie Island, north-eastern region, Antongil Bay), Mayotte and Tanzania (Mafia) coral records are single cores. The coral core names that make the composite and single records and the period each one lasts for the respective sites are given in Table 2.1.



### *2.4. Warming trends*

Warming rates are calculated for both the tropical and subtropical WIO from coral SST, ERSSTv3 and HadSST1.1 data sets. The same SST anomalies used to calculate DHM are utilised in this section to work out the trends. Linear trend analysis (Hess et al., 2001; Azman et al., 2006) is firstly performed on an annual basis based on the common long period 1870-1995, owing to the fact that the instrumental data HadSST1.1 starts in 1870. For data sets that do not go back to 1870, the maximum length is used instead. The same period 1870-1995 is then used to analyse summer and winter trends. One season may show a higher warming trend than the other for some regions. The summer period is calculated from November to April and winter from May to October. The monthly SST data are converted into annual data by simple arithmetic addition in order to calculate the annual linear

trend analysis. It should be noted that there are no monthly data for Kenya and thus no seasonal trend was performed. The gradient obtained after plotting the SST anomalies versus years is equal to the warming trend per year. To obtain the warming trend for the period 1870-1995, the gradient is multiplied by the total number of years for this period, which amounts to 126 years. A positive gradient implies warming whereas a negative gradient means cooling. A Mann-Whitney U-Test (for small sample sizes and independent samples [4 tropical and 7 subtropical data]) is used to find out if the warming trend is significantly higher in the tropical region compared to the subtropical region for each data set. Lord's Range test (for comparing very small samples with 2-4 measurements [3 tropical and 3 subtropical data]) and a Wilcoxon Matched Paired Sample Test (small sample size [7 tropical and 7 subtropical data]) are applied to investigate whether the summer trends are higher than the winter trends for each respective data set.. The test results are shown in Appendix (Section 6.3).



### *2.5. Wavelet analysis*

Wavelet analysis has been commonly used as a tool for the investigation of localised variations of power in long time series (Torrence and Compo, 1998) and in this study, the wavelet power spectra are done by using the online software (*available at*: http://paos.colorado.edu/research/wavelets/) developed by Torrence and Compo (1998), which allows the calculation of significance levels of the wavelet moduli. Wavelet analysis has been applied on coral records in the WIO by a few investigators such as Pfeiffer et al. (2004a, b) and Zinke et al. (2004). Annual SST anomalies (relative to the period 1961-1990) derived from coral proxy data are used to generate wavelet power spectra. The latter are computed for 3 sites in the tropical region and 3 sites in the subtropical region in the WIO. The 3 tropical sites are Seychelles-Chagos combination, Tanzania and Kenya, and the 3 subtropical sites are Mayotte, Madagascar (south-western region) and Rodrigues Island. Wavelet analysis is done using the Morlet Wavelet and the confidence levels (90%) are performed against a red noise spectrum chosen from the software. Owing to the fact that that the time series of the coral records are finite in length, errors will occur at the beginning and end of the wavelet power spectra generated (Torrence and Compo, 1998). Before performing the wavelet transform, the end of the time series will be padded with zeroes, which will introduce discontinuities at the endpoints (Torrence and Compo, 1998). As such, the amplitude near the edges will decrease when more zeroes are added as we go to larger scales (Torrence and Compo, 1998). This will be represented as the cone of influence (demarcated as stippled lines) on the wavelet power spectra.

Wavelets will also be performed for the El Niño-Southern Oscillation Index (Nino3.4), Indian Ocean Dipole Mode Index (DMI) and the PDO Index. This will potentially help in linking the periods of the significant variability for the six sites in the WIO with these climate indices and hence providing possible interpretations. The Niño3.4 quantifies the amplitude of an ENSO event by averaging the monthly SST over the tropical Pacific bounded by 5°N-5°S and 120°W-170°W. The PDO Index refers to the leading PC of the monthly SST anomalies from the North Pacific Ocean. As for the DMI which measures the intensity of the IOD, it refers to the SST anomaly difference between the tropical WIO (50°E-70°E, 10°S-10°N) and the tropical south-eastern Indian Ocean (90°E-110°E, 10°S-equator).

**Table 2.1. Site, coral core name and period of each record in the tropical and subtropical WIO used for the calculation of DHM.**

| | Site | Core name | Period |
|---|---|---|---|
| Tropical | Seychelles | NEP | 1840-1994 |
| | | BVB | 1846-1995 |
| | | SA | 1990-2003 |
| | Chagos | GIM | 1880-1995 |
| | | PIE | 1950-1995 |
| | | COI5 | 1950-1995 |
| | Seychelles-Chagos | Combination of 6 above cores from both Seychelles and Chagos | 1841-2002 |
| Subtropical | Reunion Is. | LaRe1 | 1835-1995 |
| | | LaRe Jens | 1978-2003 |
| | | St. Rose | 1987-2003 |
| | Rodrigues Is. | Totor | 1765-2005 |
| | | Cabri | 1945-2006 |
| | Madagascar (St. Marie Island) | STM2 | 1955-2006 |
| | Madagascar (south-western region) | Ifaty-4 | 1660-2007 |
| | Madagascar (north-eastern region) | Big Mum | 1951-2007 |
| | Madagascar (Antongil Bay) | MAS1 | 1966-2006 |
| | | ANDRA | 1970-2006 |
| | | IFAHO | 1980-2006 |
| | Mayotte | AND3 | 1881-2006 |
| | Tanzania | Mafia | 1897-1997 |

## 3.0 Results

### *3.1. Correlation of coral records with satellite sea surface temperature (SST) data*

The relationship between the coral proxy data and AVHRR SST is investigated in this section. This relationship is examined on bimonthly or monthly and annual time scales (Table 3.1). Coral core(s) taken at one site contain(s) either $\delta^{18}O$ or Sr/Ca, or both tracers. At sites where both geochemical proxies are available, linear correlation with AVHRR SST is carried out with the 2 tracers (Table 3.1). Some sites like Madagascar and Reunion Island have more than 1 coral record from the same location and also contain a composite coral record, which is computed by averaging two or more individual records from this location (Table 1.1; Table 3.1). Furthermore, for each correlation, the regression equation and the linear correlation coefficient are reported. The gradient of nearly all the regression equations is negative, likewise for most of the correlation coefficient values. The regression equation is in the form: $y = a(\pm SE) - b(\pm SE)X$, where a = y-intercept, b = slope, $y = \delta^{18}O$ (‰ $^{o}C^{-1}$) or Sr/Ca (mmol/mol $^{o}C^{-1}$) and X = SST ($^{o}C$). An example of a regression is given in Appendix (Figure 6.1; Table 6.1).

Out of 4 bimonthly records investigated, only that from Chagos shows no significant correlation at 5 % level with AVHRR SST. On monthly time scales, all coral data correlate significantly with AVHRR SST. It is noteworthy to point out that the linear correlation coefficient values on monthly time scales have higher correlation values compared to annual data. On the annual time scales, most coral data do not correlate significantly with AVHRR SST at 5 % level, with the exception of 2 cores from Madagascar and 2 other cores from Reunion Island, both from subtropical WIO region (Table 3.1). Slightly different correlation coefficients were found with records taken from Antongil Bay, Madagascar, notably the cores MAS1, ANDRA and IFAHO. Moreover, the composite record 'Ifaty-comp' from Madagascar performed better (with a higher correlation coefficient) on both monthly and annual time scales than the individual record 'Ifaty-4'. From Reunion Island, the individual record 'St. Rose' did better than the composite record 'LaRe-comp' on monthly time scale, whereas on annual time scale, the individual record 'LaRe-Jens' performed better than any other record.

Concerning the uncertainties( ±SE) in the slopes, they vary from ±0.01 to ±0.03 (with the exception of ±0.88 for Seychelles from the core NEP) for the regression slopes for the monthly $\delta^{18}O$ data and from ±0.01 to ±0.37 for annual $\delta^{18}O$ data. There was practically any uncertainty in the regression slopes for the monthly Sr/Ca data (except ±0.01 for Chagos from the core GIM), but the uncertainties do vary from ±0.02 to ±0.08 for the annual Sr/Ca data. In fact, the uncertainties in the slopes were found to be lower with monthly data compared to annual data.

**Table 3.1. Linear correlation coefficients between bimonthly or monthly and annual mean coral δ18O and/or Sr/Ca and AVHRR SST for tropical and subtropical sites in the WIO.**

| | Site | Coral core | Period of correlation | Tracer | Regression equation (bimonthly) | Regression equation (monthly) | Regression equation (annual) | Linear correlation coefficient (bimonthly) | Linear correlation coefficient (monthly) | Linear correlation coefficient (annual) |
|---|---|---|---|---|---|---|---|---|---|---|
| Tropical | Seychelles | BVB | 1982-1994 | $\delta^{18}O$ | - | y =- 2.4074(±0.41) - 0.0856(±0.01)x | y =-1.6821(±4.97)- 0.1114(±0.18)x | - | **-0.68** | -0.39 |
| | | NEP | 1982-1993 | $\delta^{18}O$ | - | y =2.338(±0.62)- 0.0853(±0.02)x | y =1.357(±6.73)- 0.1202(±0.24)x | - | **-0.54** | -0.33 |
| | | Seychelles-comp | 1982-1993 | $\delta^{18}O$ | - | y = 2.357(±0.44)- 0.0859(±0.01)x | y = -1.548(±5.39)- 0.115(±0.19)x | - | **-0.67** | -0.39 |
| | Chagos | Chagos | 1982-1994 | $\delta^{18}O$ | y = - 4.1252(±1.25)- 0.0283(±0.04)x | - | y =- 2.6549(±4.70) - 0.0796(±0.16)x | -0.15 | - | -0.31 |
| | | GIM | 1982-1994 | $\delta^{18}O$ | - | y = -3.5348(±0.82)- 0.0403(±0.03)x | y = -4.6299(±7.20)- 0.0021(±0.25)x | - | **-0.22** | 0.00 |
| | | | | Sr/Ca | - | y =9.1077(±0.19)- 0.0129(±0.01)x | y = 9.1592(±1.30)- 0.0147(±0.04)x | - | **-0.29** | -0.21 |
| | Kenya | Malindi | 1982-1994 | $\delta^{18}O$ | - | - | y=-4.3693(±4.35)- 0.0077(±0.16)x | - | - | -0.032 |
| | Tanzania | Mafia | 1982-1997 | $\delta^{18}O$ | - | y=-2.2845(±0.29)- 0.0646(±0.01)x | y=-2.287(±4.24)- 0.0645(±0.01)x | - | **-0.66** | -0.23 |
| Subtropical | Mayotte | AND3 | 1982-1992 | $\delta^{18}O$ | y=-2.3688(±0.65)- 0.0948(±0.02)x | - | y= -5.3302(±3.76)+ 0.0122(±0.13)x | **-0.71** | - | 0.068 |
| | | | | Sr/Ca | y=10.1(±0.23)- 0.0475(±0.01)x | - | y=9.2592(±1.70)- 0.0171(±0.06)x | **-0.82** | - | -0.20 |
| | Madagascar | Ifaty-4 | 1982-1994 | $\delta^{18}O$ | y=-0.637(±0.46)- 0.1433(±0.02)x | - | y=-1.76(±2.69)- 0.1011(±0.10)x | **-0.88** | - | **-0.55** |
| | | | | Sr/Ca | - | y=9.9843(±0.12)- 0.0349(±0.00)x | y=9.8461(±2.04)- 0.0297(±0.08)x | - | **-0.78** | -0.25 |
| | | Ifaty-comp | 1982-2007 | Sr/Ca | - | y=10.137(±0.09)- 0.0405(±0.00)x | y=10.305(±1.00)- 0.0468(±0.04)x | - | **-0.81** | **-0.47** |
| | | MAS1 | 1982-2006 | $\delta^{18}O$ | - | y=-2.7278(±0.47)- 0.0996(±0.02)x | y=-3.3569(±5.49)- 0.0764(±0.21)x | - | **-0.54** | -0.16 |

Values in bold are significant at the 5% level.

**Table 3.1.** ***continued…***

| | | | | | | | | | | |
|---|---|---|---|---|---|---|---|---|---|---|
| **Subtropical** | Madagascar | | | Sr/Ca | - | y=9.2047(±0.11)-0.0128(±0.00)x | y=9.2936(±1.34)-0.0162(±0.05)x | - | **-0.33** | -0.14 |
| | | ANDRA | 1988-2006 | $\delta^{18}O$ | - | y=-3.0792(±0.67)-0.0795(±0.02)x | y= -6.3789(±9.78)+0.0446(±0.37)x | - | **-0.38** | 0.062 |
| | | | 1982-2006 | Sr/Ca | - | y=9.783(±0.09)-0.0323(±0.00)x | y=9.884(±1.44)-0.0362(±0.05)x | - | **-0.72** | -0.28 |
| | | IFAHO | 1982-2005 | $\delta^{18}O$ | - | y=-4.5903(±0.51)-0.0213(±0.02)x | y=-2.583(±4.05)-0.0968(±0.15)x | - | **-0.13** | -0.27 |
| | | | | Sr/Ca | - | y=8.755(±0.13)+0.0057(±0.00)x | y=9.5954(±1.01)-0.0259(±0.04)x | - | **0.13** | -0.29 |
| | | STM2 | 1982-2005 | Sr/Ca | - | y=9.7711(±0.08)-0.0383(±0.00)x | y=8.7333(±0.72)+0.0008(±0.03)x | - | **-0.84** | 0.013 |
| | | STM4 | 1982-2005 | Sr/Ca | - | y=10.211(±0.09)-0.0466(±0.00)x | y=8.883(±0.84)+0.0034(±0.03)x | - | **-0.86** | 0.047 |
| | | STM-comp | 1982-2005 | Sr/Ca | - | y=9.991(±0.07)-0.0425(±0.00)x | y=8.8082(±0.65)+0.0021(±0.02)x | - | **-0.88** | 0.037 |
| | | Big Mum | 1982-2006 | Sr/Ca | - | y=9.6848(±0.09)-0.0347(±0.00)x | y=8.9402(±0.55)-0.0071(±0.02)x | - | **-0.75** | -0.15 |
| | Reunion Is. | LaRe-1 | 1982-1994 | $\delta^{18}O$ | - | y=-1.5899(±0.35)-0.1151(±0.01)x | y=-4.55(±4.65)-0.0001(±0.18)x | - | **-0.80** | -0.00043 |
| | | | | Sr/Ca | - | y=9.7625(±0.11)-0.0361(±0.00)x | y=9.3719(±1.25)-0.0209(±0.05)x | - | **-0.81** | -0.27 |
| | | LaRe-Jens | 1982-2002 | Sr/Ca | | y=9.8329(±0.08)-0.0378(±0.00)x | y=11.129(±1.09)-0.0882(±0.04)x | - | **-0.84** | **-0.71** |
| | | St. Rose | 1988-2002 | Sr/Ca | - | y=9.9564(±0.09)-0.0464(±0.00)x | y=9.1792(±1.27)-0.0161(±0.05)x | - | **-0.88** | -0.19 |
| | | LaRe-comp | 1982-2002 | Sr/Ca | - | y=9.8336(±0.07)-0.0393(±0.00)x | y=9.9271(±1.09)-0.0429(±0.04)x | - | **-0.87** | **-0.44** |
| | Rodrigues Is. | Cabri | 1982-2005 | Sr/Ca | - | y=9.9503(±0.09)-0.0419(±0.00)x | y=9.6458(±1.10)-0.03(±0.04)x | - | **-0.79** | -0.29 |
| | | Totor | 1982-2004 | Sr/Ca | - | y=10.272(±0.09)-0.0522(±0.00)x | y=9.8565(±0.99)-0.036(±0.04)x | - | **-0.87** | -0.39 |

Values in bold are significant at the 5% level.

### *3.2. Degree Heating Month*

The DHM for Chagos is calculated from 1881 to 1995 (Figure 3.1). From the coral SST, the annual accumulated thermal stress was highest in 1983 (ENSO and positive IOD year) with a DHM value of 15.8 °C-months. The highest DHM from ERSSTv3 and HadSST1.1 are recorded in 1988 (ENSO year) with a DHM value of 5.5 °C-months and in 1992 (ENSO and negative IOD year) with a DHM value of 5.6 °C-months respectively. The magnitude of the highest annual accumulated thermal stress recorded from the coral SST is about thrice that calculated from instrumental SSTs. There is a clear increase in DHM from the late 1970's to the recent period and quite similarly, the 1890's record high DHM, which is followed closely by the early 1940's, 1958-1959 (ENSO year) and 1962-1964.



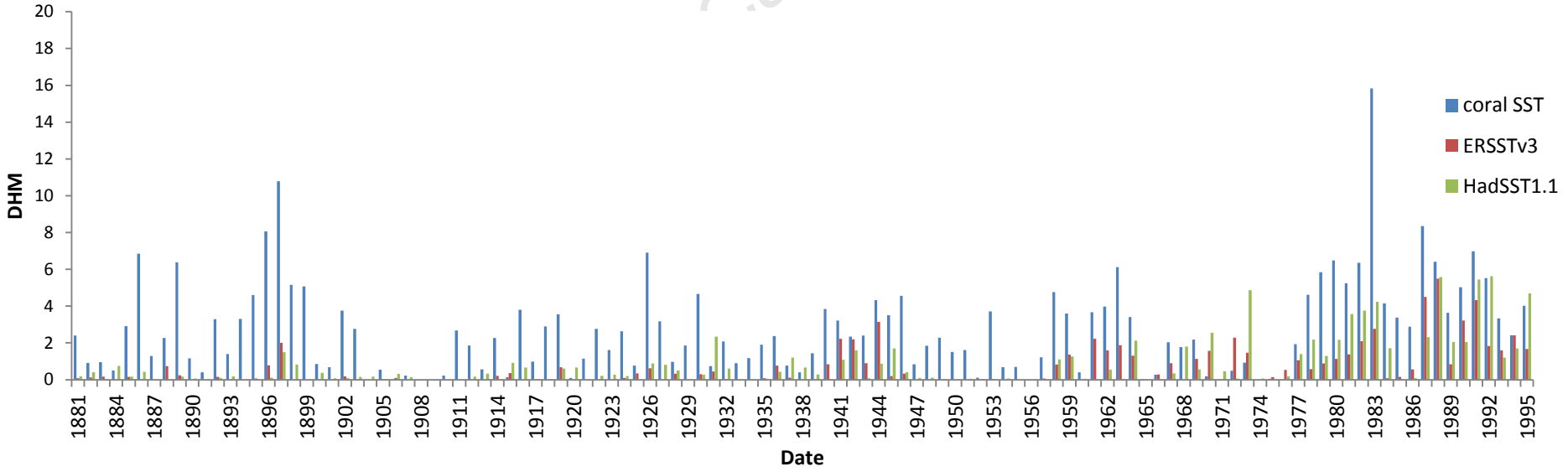


**Figure 3.1. DHM for Chagos calculated from coral SST, ERSSTv3 and HadSST1.1**

The calculated DHM for Seychelles starts in 1841 for the coral SST, 1854 for the ERSSTv3 and 1870 for HadSST1.1, and all end in 2003 (Figure 3.2). The highest accumulated stress was in 2003 (ENSO year) for coral SST with a DHM value of 17.8 °C-months, followed by 15.6 °C-months in 1998. 1998 (coinciding ENSO and negative IOD year) was the year where the highest DHM was recorded for both instrumental SSTs, with 7.1°C-months for ERSSTv3 and 7.8°C-months for HadSST1.1. Higher DHM is observed towards the end of the data set as from the 1970's. The highest accumulated thermal stress recorded by coral SST is about twice that recorded by the two instrumental SSTs. High DHM is also observed in 1877/1878 (ENSO year).



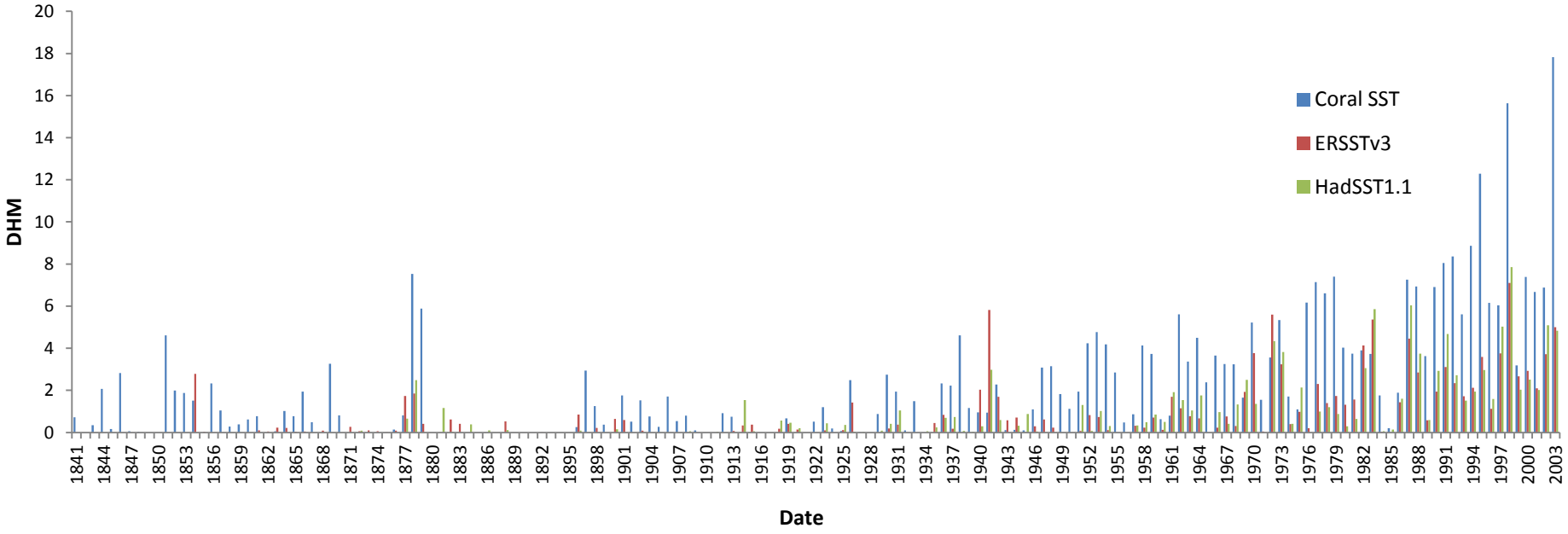


**Figure 3.2. DHM for Seychelles calculated from coral SST, ERSSTv3 and HadSST1.1**

The calculated DHM for the Seychelles-Chagos combination starts in 1841 and ends in 2002 (Figure 3.3). The year 1998, which is both an ENSO and a negative IOD year, was the one with the highest annual accumulated thermal stress as noted with the coral SST as well as with the instrumental SSTs. A DHM of 18.1 °C-months was recorded for the coral SST, 6.8 °C-months for ERSSTv3 and 9.2 °C-months for HadSST1.1.The highest DHM recorded for the coral SST is nearly thrice that for ERSSTv3 and about twice that for HadSST1.1. DHM tends to increase in magnitude since the 1960's and high DHM is further noticeable in 1877-1878 (ENSO year).



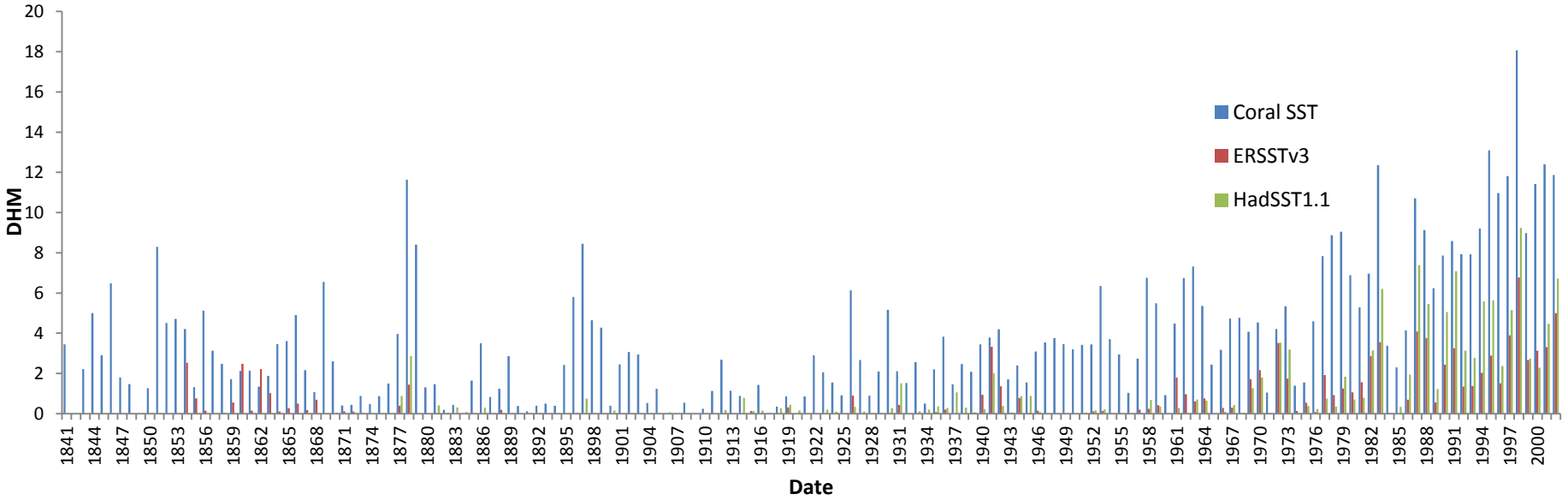


**Figure 3.3. DHM for Seychelles-Chagos calculated from coral SST, ERSSTv3 and HadSST1.1**

For Reunion Island, DHM was calculated from 1913 to 2002 (Figure 3.4) and higher thermal stress was noted in 2002 (ENSO year) with coral SST with a value of 14.0°C-months as shown in Figure 3.4. 1987 (coinciding ENSO and positive IOD year) recorded the highest DHM with both the instrumental SSTs. ERSSTv3 had a DHM of 6.1 °C-months and HadSST1.1 had a value of 6.4 °C-months during 1987. The highest annual accumulated thermal stress recorded by the coral SST is two times more than that for the two instrumental SSTs. There is an evident increase in DHM since the 1970's and high DHM is also noted in the early 1940's but of lower magnitude than for the most recent period.



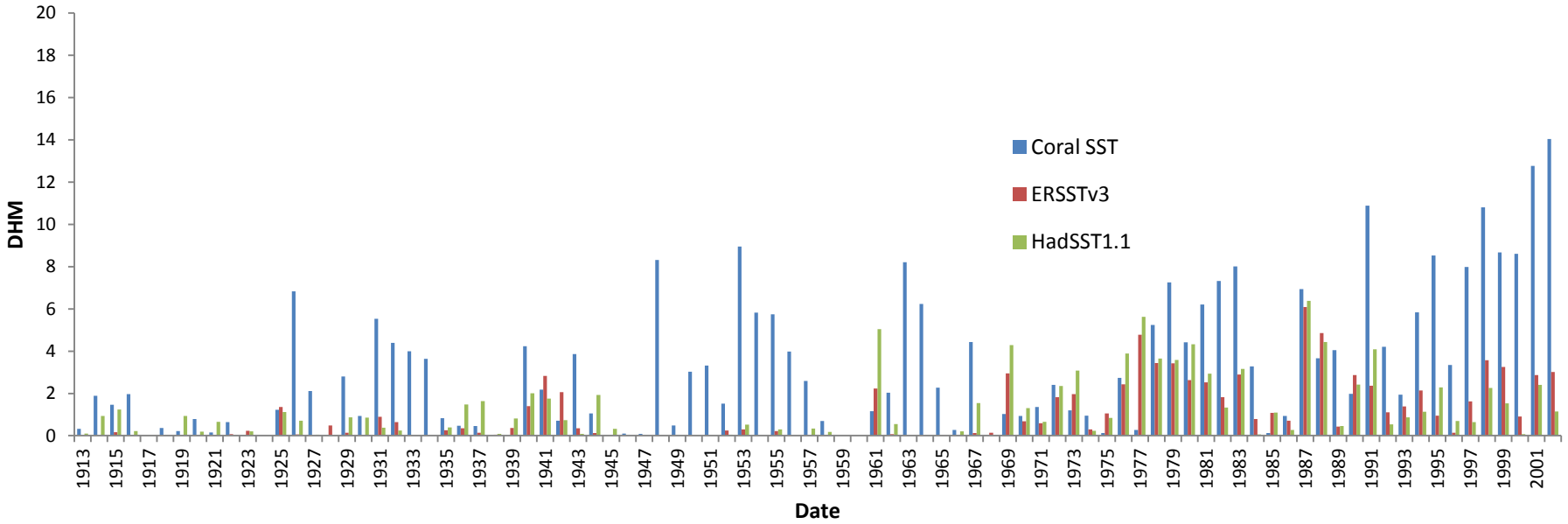


**Figure 3.4. DHM for Reunion calculated from coral SST, ERSSTv3 and HadSST1.1**

For Rodrigues Island, DHM was calculated from coral SST starting in 1782 and ending in 2005 (Figure 3.5). There is a period with relatively high SST between 1915 and 1921 with the coral SST, as highlighted in Figure 3.5 below. High DHM values occurring in this period are ignored because this period is based on only one single coral core and is too anomalous. The highest annual accumulated thermal stress for the coral SST was recorded in 1940 with a DHM value of 17.2 °C-months, followed by 2005 (ENSO year) with a DHM value of 11.9 °C-months. For ERSSTv3, the highest DHM value of 6.5 °C-months was recorded in 1987 (coinciding ENSO and positive IOD year) and that of HadSST1.1 was recorded in 1977 (positive IOD year) with a DHM value of 8.8 °C-months, followed by the year 1987 with a DHM value of 8.5 °C-months. The highest DHM values recorded by the coral SST which is about twice that recorded by the two instrumental SSTs. Since the 1970's, strong DHM values are recorded and high DHM are noted in 1939-1942 (ENSO years) period, in the late 1700's and the 1820's.

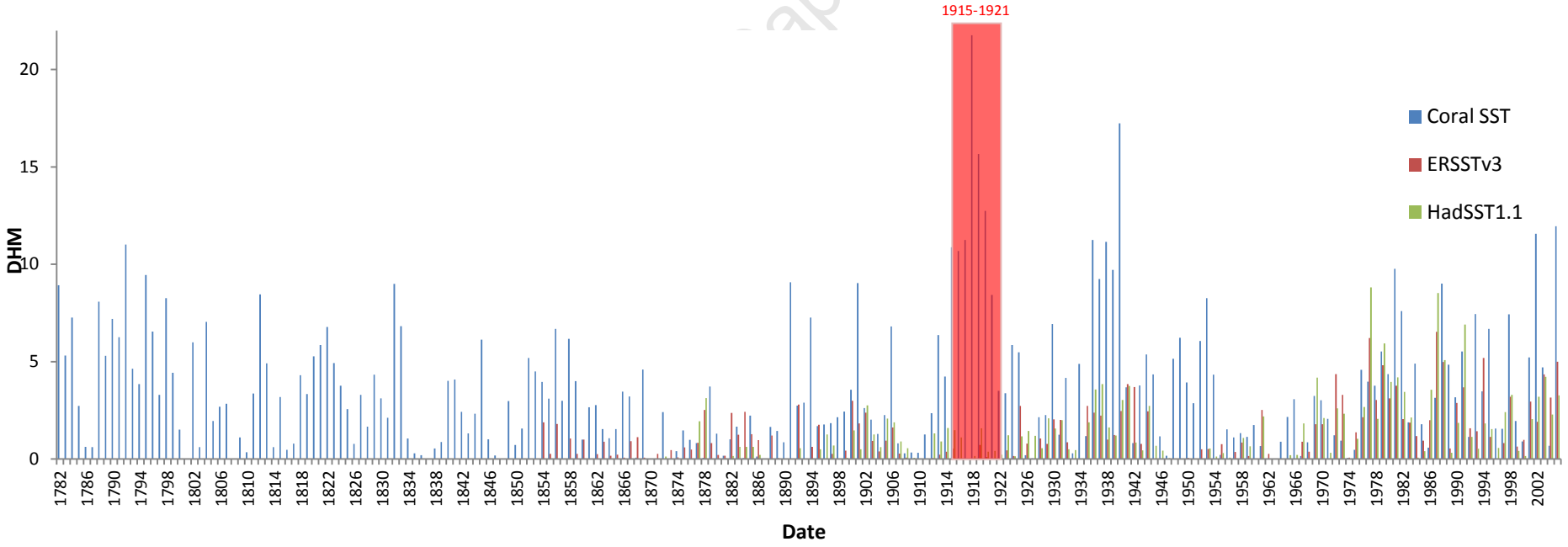


**Figure 3.5. DHM for Rodrigues calculated from coral SST, ERSSTv3 and HadSST1.1**

The annual accumulated thermal stress was calculated for St. Marie Island (Madagascar) from 1956-2005 (Figure 3.6). The highest value for the coral SST was recorded in 1988 (ENSO year) with a DHM value of 14.2 °C-months. For ERSSTv3, the highest accumulated thermal stress was noted in 1987 (coinciding ENSO and positive IOD year), with a DHM value of 5.9 °C-months, followed by 1998 (coinciding ENSO and negative IOD year) with a DHM value of 5.2 °C-months. Concerning HadSST1.1, the highest value was recorded in 1987 (coinciding ENSO and positive IOD year) with a DHM value of 5.0 °C-months. The highest DHM values recorded by the coral SST is about 2-3 times greater than the values recorded by the two instrumental SSTs. Similar to other sites, higher DHM values are observed as from the 1970's up to the most recent period.



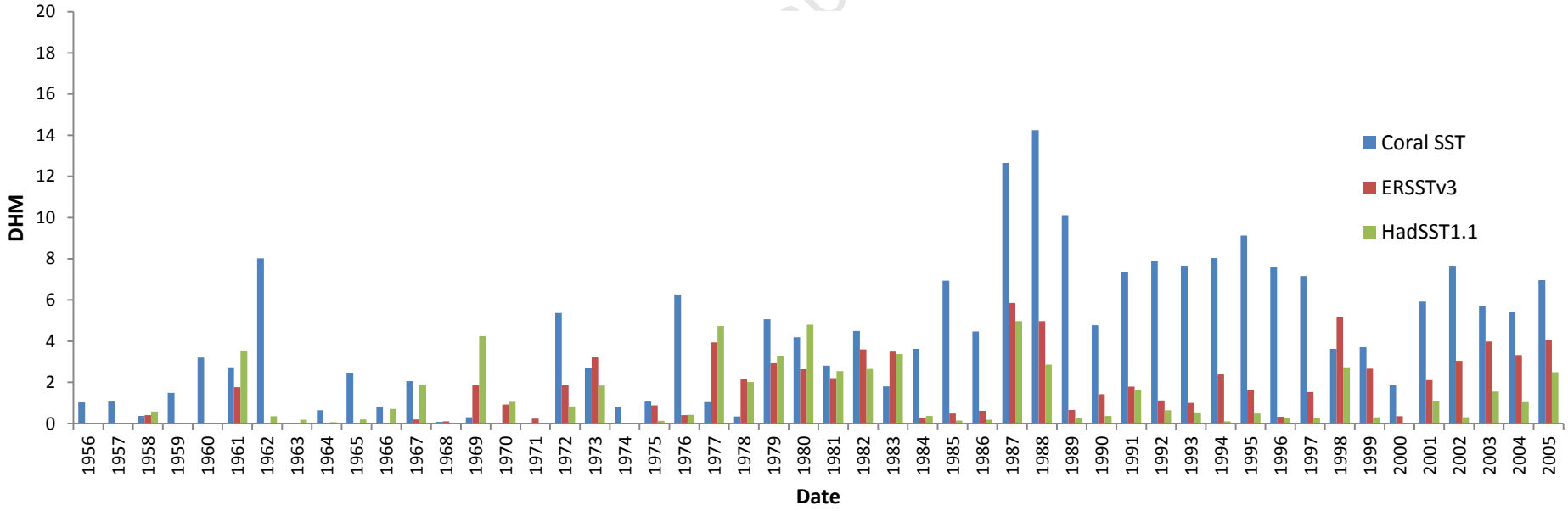


**Figure 3.6. DHM for St. Marie Island (Madagascar) calculated from coral SST, ERSSTv3 and HadSST1.1**

DHM was calculated for the south-western region of Madagascar with the composite core Ifaty-4 from 1800 to 2007 (Figure 3.7). The highest annual accumulated thermal stress for the coral SST was noted in 1856 with a DHM value of 17.0 °C-months, followed by 1896 with a DHM value of 13.6 °C-months. The highest value calculated for ERSSTv3 was in 1893 with a DHM value of 7.4 °C-months, followed by 2007 (ENSO year) with a DHM value of 6.7 °C-months. The thermal stress was maximally recorded for HadSST1.1 in 1992 (negative IOD year) with a DHM value of 10.8 °C-months. DHM values increase from the 1970's and during the earlier period, strong DHM was recorded during the period 1939-1942 and interestingly during the 1800's, particularly during 1809-1812, 1824/1825, 1856-1860 and 1890's.



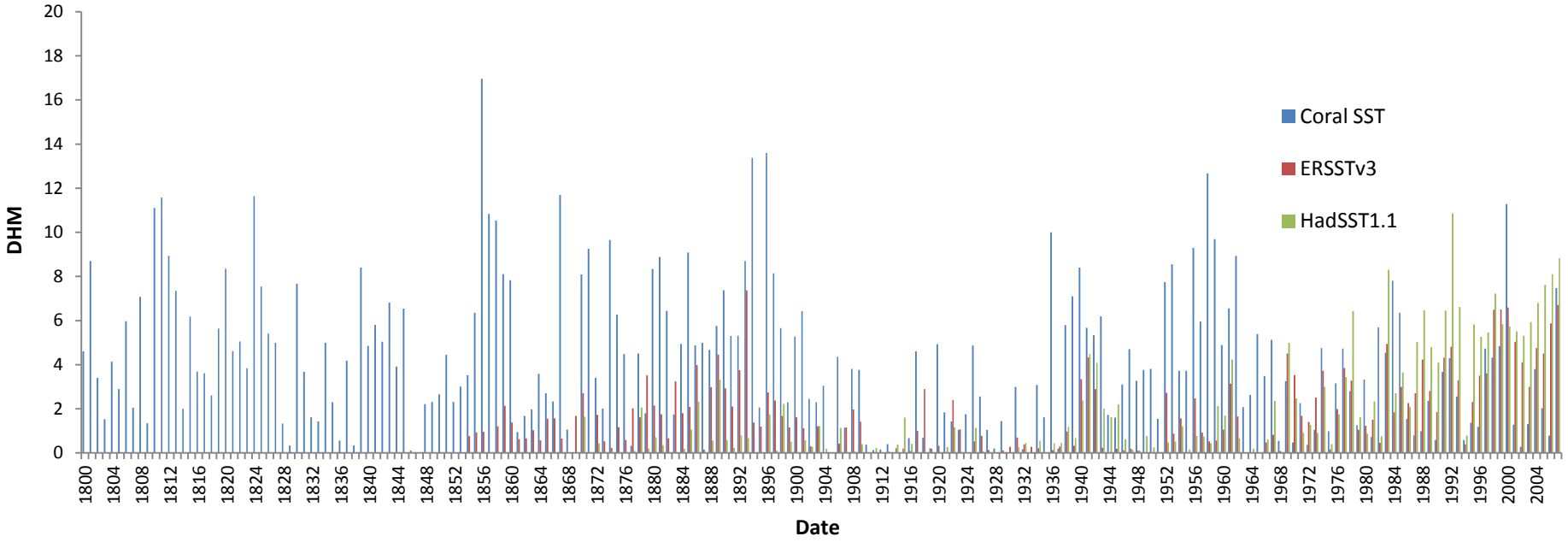


**Figure 3.7. DHM for the south-western region of Madagascar calculated from coral SST, ERSSTv3 and HadSST1.1**

The DHM for the north-eastern region of Madagascar from the Big Mum core was calculated from 1952-2006 (Figure 3.8). Coral SST recorded the highest annual accumulated thermal stress in 1973 (ENSO year) with a DHM value of 7.1 °C-months, while with the instrumental SSTs, the highest DHM was noted in 1987 (coinciding ENSO and positive IOD year) with ERSSTv3 with a value of 5.8 °C-months and in 1983 (positive IOD year) with HadSST1.1 with a value of 6.2 °C-months. The years 1972 (coinciding ENSO and positive IOD year), 1973, 1982 (coinciding ENSO and positive IOD year), 1983 (positive IOD year), 1987 (coinciding ENSO and positive IOD year), 1988 (ENSO year), 1998 (coinciding ENSO and negative IOD year) and 2005 (ENSO year) recorded high DHM values whose magnitudes are in fact a little lower than the other sites.



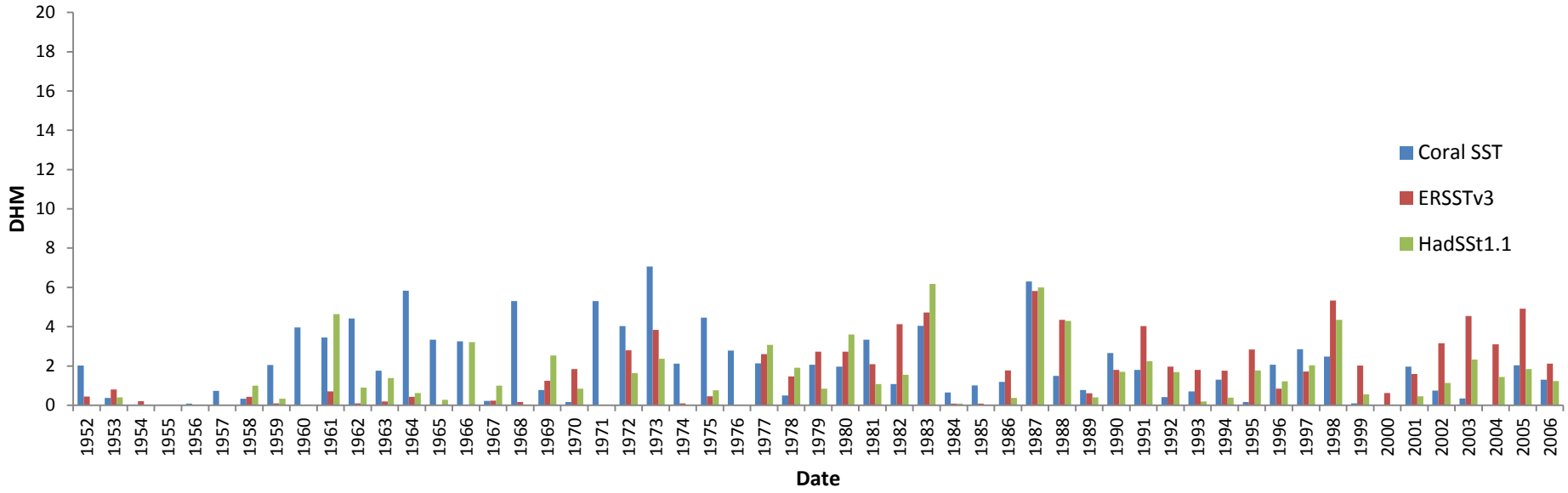


**Figure 3.8. DHM for the north-eastern region of Madagascar calculated from coral SST, ERSSTv3 and HadSST1.1**

For Antongil Bay, DHM was calculated from 3 coral SSTs, obtained from 3 cores situated a few kilometres apart from each other, and from the 2 instrumental SSTs from 1966-2006 (Figure 3.9). The year 1997 (coinciding ENSO and positive IOD year) recorded the highest DHM with MAS1 with a value of 10.9 °C-months and 2006 (coinciding ENSO and positive IOD year) recorded the highest DHM with ANDRA and IFAHO with 22.1 °C-months and 10.5 °C-months respectively. ERSSTv3 had the highest DHM value in 1987 (coinciding ENSO and positive IOD year) with 5.6 °C-months and HadSST1.1 recorded the highest value in 1977 (positive IOD year) with 7.0 °C-months. High DHM values were also observed during the early 1980's, 1987/1988, 1990/1991, 1998 and 2001-2006.



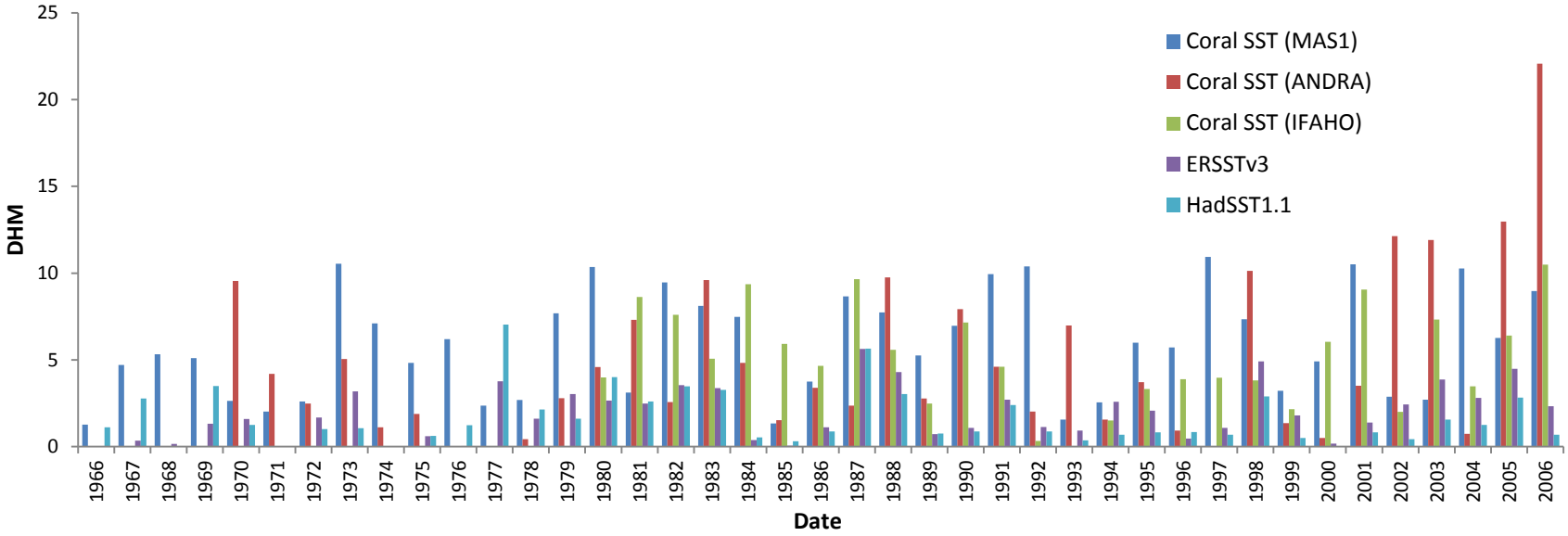


**Figure 3.9. DHM for the Antongil Bay region of Madagascar calculated from 3 coral SSTs, ERSSTv3 and HadSST1.1**

DHM for Mayotte was performed from 1882-2006 (Figure 3.10) and the values were relatively lower than the tropical sites analysed. The year 1951 had the highest DHM with coral SST with 3.6 °C-months, followed closely by 1944 with 3.5 °C-months. ERSSTv3 recorded the maximum DHM value of 1.6 °C-months in 2001 (negative IOD year), 1995 and 1981 and HadSST1.1 recorded the highset DHM value in 1996 (negative IOD year) and 1994 (positive IOD year) with 1.6 °C-months. There is a clear increase in DHM since the early 1970's and high DHM values was further observed in the 1950's. (*Note: coral SST ends in 1992 for this data set*)



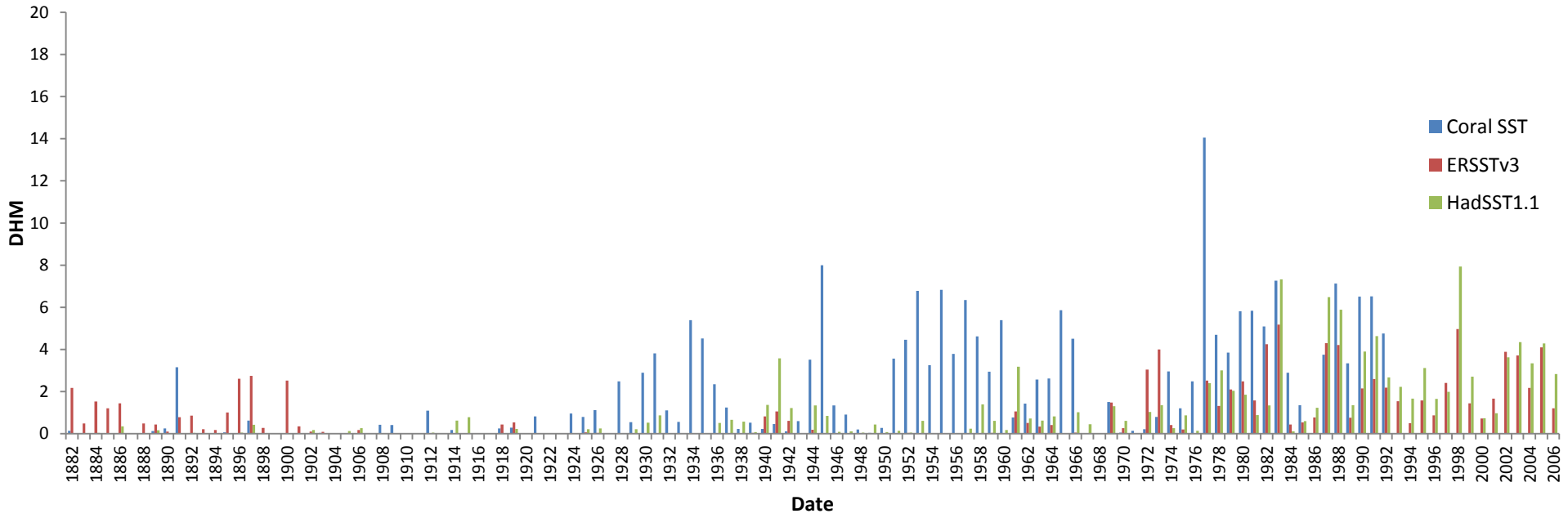


**Figure 3.10. DHM for Mayotte calculated from coral SST, ERSSTv3 and HadSST1.1**

The annual accumulated thermal stress was determined for Tanzania from 1897 to 1997 (Figure 3.11). The maximum DHM calculated with coral SST was noted in 1940 and 1977 (positive IOD year) with a DHM value of 7.8 °C-months. For ERSSTv3, the highest value was recorded in 1983 (positive IOD year) with a DHM value of 4.9 °C-months and for HadSST1.1, a DHM value of 5.8 °C-months was maximally recorded in 1983 (positive IOD year). The DHM values for this subtropical site are relatively lower compared to the other tropical and other subtropical sites. Yet, it is evident that DHM values increase from the 1970's and that high DHM is observed also during the 1939-1942 period.



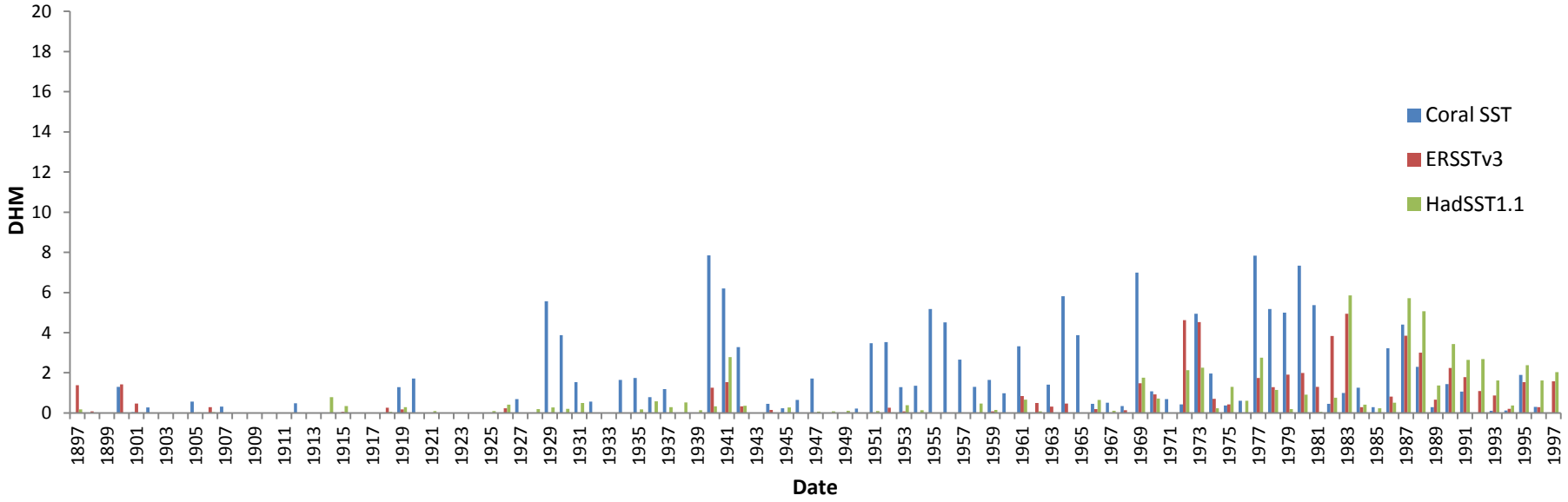


**Figure 3.11. DHM for Tanzania calculated from coral SST, ERSSTv3 and HadSST1.1**

**Table 3.2. Year with highest DHM value, including whether it is a major ENSO and IOD year or not, and the general historical SST variability for each different SST data from 3 tropical and 8 subtropical sites.**

| | Site | SST data | Year with highest DHM value | Major ENSO year | IOD year | General historical SST variability |
|---|---|---|---|---|---|---|
| Tropical | Chagos | Coral SST | 1983 | Yes | Yes (positive) | High |
| | | ERSSTv3 | 1988 | Yes | No | |
| | | HadSST1.1 | 1992 | Yes | Yes (negative) | |
| | Seychelles | Coral SST | 2003 | Yes | No | Low to moderate |
| | | ERSSTv3 | 1998 | Yes | Yes (negative) | |
| | | HadSST1.1 | 1998 | Yes | Yes (negative) | |
| | Seychelles-Chagos | Coral SST | 1998 | Yes | Yes (negative) | High |
| | | ERSSTv3 | 1998 | Yes | Yes (negative) | |
| | | HadSST1.1 | 1998 | Yes | Yes (negative) | |
| Subtropical | Reunion Is. | Coral SST | 2002 | Yes | No | Low to moderate |
| | | ERSSTv3 | 1987 | Yes | Yes (positive) | |
| | | HadSST1.1 | 1987 | Yes | Yes (positive) | |
| | Rodrigues Is. | Coral SST | 1940 | No | No | Moderate to high |
| | | ERSSTv3 | 1987 | Yes | Yes (positive) | |
| | | HadSST1.1 | 1977 | No | Yes (positive) | |
| | Madagascar (St. Marie Island) | Coral SST | 1988 | Yes | No | Low to moderate |
| | | ERSSTv3 | 1987 | Yes | Yes (positive) | |
| | | HadSST1.1 | 1987 | Yes | Yes (positive) | |
| | Madagascar (south-western region) | Coral SST | 1856 | No | - | Moderate to high |
| | | ERSSTv3 | 1893 | No | No | |
| | | HadSST1.1 | 1992 | Yes | Yes (negative) | |

**Table 3.2.** ***continued…***

| | | | | | | |
|---|---|---|---|---|---|---|
| | Madagascar (north-eastern region) | Coral SST | 1973 | Yes | No | Low |
| | | ERSSTv3 | 1987 | Yes | Yes (positive) | |
| | | HadSST1.1 | 1983 | Yes | Yes (positive) | |
| | Madagascar (Antongil Bay) | Coral SST | 1997, 2006 | Yes | Yes (positive) | Low to moderate |
| | | ERSSTv3 | 1987 | Yes | Yes (positive) | |
| | | HadSST1.1 | 1977 | No | Yes (positive) | |
| | Mayotte | Coral SST | 1951 | No | No | Low |
| | | ERSSTv3 | 2001 | No | Yes (negative) | |
| | | HadSST1.1 | 1996, 1994 | No, No | Yes (negative), Yes (positive) | |
| | Tanzania | Coral SST | 1940, 1977 | No, No | No, Yes (positive) | Low |
| | | ERSSTv3 | 1983 | Yes | Yes (positive) | |
| | | HadSST1.1 | 1983 | Yes | Yes (positive) | |

Table 3.2 summarises the DHM exercise by listing the year which recorded the highest DHM value for each SST data, and showing whether it is an ENSO and an IOD year. The classification for the ENSO and IOD years is based on Saji et al. (1999), Hong et al. (2008), Meyers et al. (2007) for the earlier period before 1960, and Ummenhofer et al. (2009) for the recent years after 2001. Lots of differences were noted in the classification of the ENSO and IOD years from the above listed authors, making this task quite problematic. In addition, the general historical SST variability is given for each site based on the DHM time series (Figures 3.1-3.11).

### *3.3. Warming trends*

Between 1870 and 1995, the annual average SSTs warmed for the 4 tropical sites as observed with the coral SST and the 2 instrumental SSTs (Table 3.3).An example of a regression graph is shown in Appendix (Figure 6.2; Table 6.2). This warming was significant (at the 5% level) in all the tropical sites, except for Kenya with coral SST. For the 7 subtropical sites, coral SST significantly cooled off south-

western Madagascar and warming was noted for the 6 other regions and with coral and instrumental SSTs. Yet, warming was significant (at the 5% level) for 4 sites with coral SST, 5 sites with ERSSTv3 and 4 sites with HadSST1.1. The average warming was observed to be higher in the tropical sites compared to the subtropical sites. Mann-Whitney U-Test however indicates that warming was significantly higher ($p<0.05$) in the tropical sites compared to the subtropical sites with ERSSTv3 and HadSST1.1, but with coral SST, warming in the tropical sites was not significantly higher ($p>0.05$) compared to the subtropical sites. The test results are shown in Appendix (Table 6.3).

Warming rather than cooling was predominantly observed both for the tropical and subtropical regions during the period 1870-1995. The magnitude of the warming rates recorded by the coral SST varies between the different sites in the tropics as well as the subtropics and does not correspond with that recorded from the instrumental SSTs. The linear annual trend analysis (Table 3.3) shows that for the tropical region, the highest warming rate was recorded with coral SST at Seychelles with a value of +1.51 $^{o}$C, with ERSSTv3 at both Seychelles and Kenya with a value of +0.81 $^{o}$C and with HadSST1.1 at Kenya with a value of +0.74 $^{o}$C. A relatively low warming rate with a value of +0.31 $^{o}$C was observed for Kenya with coral SST.

For the subtropical region, St. Marie Island (Madagascar) recorded the highest warming rate with a value of +1.28 $^{o}$C with coral SST, the north-east region of Madagascar recorded the highest trend with a value of +0.69 $^{o}$C with ERSSTv3 and Mayotte recorded the highest value of +0.53 $^{o}$C with HadSST1.1. Significant cooling with a value of -0.49 $^{o}$C with coral SST, a very low warming rate of +0.07 $^{o}$C with ERSSTv3 and a significant warming rate of +0.50 $^{o}$C with HadSST1.1 were recorded in the south-western region of Madagascar during 1870-1995. In general, relatively low warming rate was recorded at Madagascar in the north-eastern region, Antongil Bay and St. Marie Island for the subtropical sites.

Analysing the summer trends for 3 tropical sites and 7 subtropical sites (Table 3.4) between 1870 and 1995 indicate that warming was significant (at the 5% level) in all the 3 tropical sites with coral SST and the 2 instrumental SSTs. With coral SST, warming was significant (at the 5% level) in only 3 sites in the subtropical region and cooling was observed in south-western Madagascar which was not significant (at the 5% level). Warming was significant (at the 5% level) for 5 sites with ERSSTv3 and for 4 sites with HadSST1.1 in the subtropical region. The annual average warming was observed to be higher in the tropical sites compared to the subtropical sites but Mann-Whitney U-Test shows that this warming was significantly higher ($p<0.05$) in the tropical region compared to the subtropical region only with ERSSTv3, whereas it was not significantly higher ($p>0.05$) in the tropical region

compared to the subtropical region with coral SST and HadSST1.1. The test results are shown in Appendix (Table 6.4).

For the summer period in the tropics, Seychelles had the highest warming trend with coral SST and ERSSSTv3 with a value of +1.45 $^{o}$C and +0.74 $^{o}$C respectively, while the highest trend with HadSST1.1 was recorded by Tanzania with a value of +0.64 $^{o}$C. For the subtropical region, Mayotte recorded the highest warming trends with coral SST and HadSST1.1 with the respective values of +1.04 $^{o}$C and +0.52 $^{o}$C while the north-eastern region of Madagascar had the highest trend with ERSSTv3 with a value of +0.51 $^{o}$C. Similar to the annual linear trend analysis (Table 3.3), the south-western region of Madagascar showed a cooling trend (which is not significant at the 5% significant level) for the summer period in the subtropical WIO with a value of -0.34 $^{o}$C.

For the winter trends, warming was significant (at the 5% level) for only 2 of the 3 tropical sites with coral SST whereas it was significant (at the 5% level) for all 3 tropical sites with the 2 instrumental SSTs (Table 3.5). Warming was significant (at the 5% level) for 4 sites with both coral SST and ERSSTv3 and 5 sites with HadSST1.1 in the subtropical region. Cooling was recorded with coral SST for north-eastern and south-western Madagascar sites but it was significant (at the 5% level) only at the south-western site.

The annual average warming for the winter period was higher in the tropical region compared to the subtropical region, yet Mann-Whitney U-Test reveals that warming was in fact not significantly ($p>0.05$) higher in the tropical region than in the subtropical region. The test results are given in Appendix (Table 6.5). When comparing the summer and winter trends for the tropical region with Lord's Range Test, warming was not significantly higher ($p>0.05$) in summer than in winter with coral SST as well as with the instrumental SSTs. Test results are shown in Appendix (Table 6.6). For the subtropical region, Wilcoxon Matched Paired Sample Test shows that warming was significantly higher ($p<0.05$) in summer than in winter only with HadSSt1.1, while warming in summer was not significantly higher ($p<0.05$) than in winter with coral SST and ERSSTv3. The test results are given in Appendix (Table 6.7).

For the tropical WIO, the highest trends recorded for winter period were from the same sites as those for summer period, with Seychelles having the maximum warming rates with coral SST and ERSSTv3 with the respective values of +1.55 $^{o}$C and +0.88 $^{o}$C and Tanzania with a value of 0.68 $^{o}$C with HadSST1.1. For the subtropics, the highest warming trend with coral SST was recorded by St. Marie Island (Madagascar) with a value of +1.40 $^{o}$C, with ERSSTv3 by the north-eastern region of Madagascar with a value of +0.86 $^{o}$C and with HadSST1.1 by the south-western region of Madagascar

with a value of +0.54 $^{o}$C. Surprisingly, the latter region showed a significant cooling trend of -0.63 $^{o}$C with coral SST for the same winter period. Antongil Bay from Madagascar also experienced a cooling trend of -0.62 $^{o}$C with coral SST, but this cooling was not significant at the 5 % significant level and the instrumental SSTs further recorded relatively low warming trends.

**Table 3.3. Linear trend analysis of the mean annual coral records, ERSSTv3 and HadSST1.1 data for 4 tropical and 7 subtropical sites in the WIO for the period 1870-1995**

| | Site | Core name | Period (no. of years) | Coral record | | | ERSSTv3 | | | HadSST1.1 | | |
|---|---|---|---|---|---|---|---|---|---|---|---|---|
| | | | | $R^2$ | *p* | SST change (°C) | $R^2$ | *P* | SST change (°C) | $R^2$ | *p* | SST change (°C) |
| **Tropical** | Seychelles | Composite (BVB, NEP, SA) | 1870-1995 (126) | **0.54** | **<0.00** | **+1.51** | **0.43** | **<0.00** | **+0.81** | **0.43** | **<0.00** | **+0.59** |
| | Chagos | Composite (GIM, PIE, COI5) | 1881-1995 (115) | **0.07** | **<0.00** | **+0.41** | **0.43** | **<0.00** | **+0.61** | **0.30** | **<0.00** | **+0.47** |
| | Kenya | Mal 96-1 | 1870-1995 (126) | 0.03 | 0.04 | +0.31 | **0.42** | **<0.00** | **+0.81** | **0.52** | **<0.00** | **+0.74** |
| | Tanzania | Mafia | 1897-1995 (99) | **0.31** | **<0.00** | **+1.05** | **0.45** | **<0.00** | **+0.69** | **0.54** | **<0.00** | **+0.66** |
| | **Average** | | | | | +0.82 | | | +0.73 | | | +0.61 |
| **Subtropical** | Mayotte | AND3 | 1882-1995 (114) (to 1993 for coral record) | **0.34** | **<0.00** | **+0.96** | **0.12** | **<0.00** | **+0.34** | **0.41** | **<0.00** | **+0.53** |
| | Madagascar (NE region) | Big Mum | 1952-1995 (44) | 0.03 | 0.24 | +0.23 | **0.50** | **<0.00** | **+0.69** | 0.13 | 0.02 | +0.30 |
| | Madagascar (Antongil Bay) | MAS1 | 1966-1995 (30) | 0.04 | 0.30 | +0.28 | 0.19 | 0.01 | +0.35 | 0.02 | 0.47 | +0.12 |
| | Madagascar (St. Marie Is) | STM2 | 1956-1995 (40) | **0.47** | **<0.00** | **+1.28** | **0.45** | **<0.00** | **+0.64** | 0.09 | 0.06 | +0.24 |
| | Madagascar (SW region) | Ifaty-4 | 1870-1995 (126) | **0.06** | **<0.00** | **-0.49** | 0.01 | 0.37 | +0.07 | **0.19** | **<0.00** | **+0.50** |
| | Reunion Is. | Composite (LaRe-1, LaRe-Jens, St. Rose) | 1913-1995 (83) | **0.17** | **<0.00** | **+0.69** | **0.30** | **<0.00** | **+0.55** | **0.17** | **<0.00** | **+0.39** |
| | Rodrigues Is. | Composite (Totor, Cabri) | 1870-1995 (126) | **0.15** | **<0.00** | **+0.80** | **0.13** | **<0.00** | **+0.39** | **0.15** | **<0.00** | **+0.40** |
| | **Average** | | | | | +0.53 | | | +0.43 | | | +0.35 |

Values in bold are significant at 5% level

**Table 3.4. Linear trend analysis of coral records, ERSSTv3 and HadSST1.1 data for 3 tropical and 7 subtropical sites in the WIO during summer for the period 1870-1995.**

| | Site | Core name | Period (no. of years) | Coral record | | | ERSSTv3 | | | HadSST1.1 | | |
|---|---|---|---|---|---|---|---|---|---|---|---|---|
| | | | | $R^2$ | $p$ | SST change (°C) | $R^2$ | $P$ | SST change (°C) | $R^2$ | $p$ | SST change (°C) |
| **Tropical** | Seychelles | Composite (BVB, NEP, SA) | 1870-1995 (126) | **0.43** | **<0.00** | **+1.45** | **0.36** | **<0.00** | **+0.74** | **0.33** | **<0.00** | **+0.63** |
| | Chagos | Composite (GIM, PIE, COI5) | 1881-1995 (115) | **0.09** | **<0.00** | **+0.56** | **0.33** | **<0.00** | **+0.60** | **0.19** | **<0.00** | **+0.39** |
| | Kenya | Mal 96-1 | *No monthly data available* | | | | | | | | | |
| | Tanzania | Mafia | 1897-1995 (99) | **0.22** | **<0.00** | **+1.1** | **0.37** | **<0.00** | **+0.65** | **0.44** | **<0.00** | **+0.64** |
| | **Average** | | | | | +1.04 | | | +0.66 | | | +0.55 |
| **Subtropical** | Mayotte | AND3 | 1882-1995 (114) (to 1993 for coral record) | **0.32** | **<0.00** | **+1.04** | **0.10** | **<0.00** | **+0.33** | **0.33** | **<0.00** | **+0.52** |
| | Madagascar (NE region) | Big Mum | 1952-1995 (44) | 0.00 | 0.65 | +0.09 | **0.36** | **<0.00** | **+0.51** | 0.05 | 0.12 | +0.19 |
| | Madagascar (Antongil Bay) | MAS1 | 1966-1995 (30) | 0.16 | 0.02 | +1.12 | 0.17 | 0.02 | +0.31 | 0.02 | 0.41 | +0.14 |
| | Madagascar (St. Marie Is) | STM2 | 1956-1995 (40) | **0.38** | **<0.00** | **+1.14** | **0.40** | **<0.00** | **+0.50** | 0.04 | 0.19 | +0.16 |
| | Madagascar (SW region) | Ifaty-4 | 1870-1995 (126) | 0.02 | 0.08 | -0.34 | 0.00 | 0.43 | +0.08 | **0.13** | **<0.00** | **+0.45** |
| | Reunion Is. | Composite (LaRe-1, LaRe-Jens, St. Rose) | 1913-1995 (83) | **0.12** | **<0.00** | **+0.59** | **0.21** | **<0.00** | **+0.45** | **0.09** | **<0.00** | **+0.26** |
| | Rodrigues Is. | Composite (Totor, Cabri) | 1870-1995 (126) | 0.04 | 0.02 | +0.46 | **0.10** | **<0.00** | **+0.39** | **0.09** | **<0.00** | **+0.33** |
| | **Average** | | | | | +0.58 | | | +0.37 | | | +0.29 |

Values in bold are significant at 5% level

**Table 3.5. Linear trend analysis of coral records, ERSSTv3 and HadSST1.1 data for 3 tropical and 7 subtropical sites in the WIO during winter for the period 1870-1995.**

| | Site | Core name | Period (no. of years) | Coral record | | | ERSSTv3 | | | HadSST1.1 | | |
|---|---|---|---|---|---|---|---|---|---|---|---|---|
| | | | | $R^2$ | *p* | SST change (°C) | $R^2$ | *P* | SST change (°C) | $R^2$ | *p* | SST change (°C) |
| **Tropical** | Seychelles | Composite (BVB, NEP, SA) | 1870-1995 (126) | **0.51** | **<0.00** | **+1.55** | **0.36** | **<0.00** | **+0.88** | **0.31** | **<0.00** | **+0.53** |
| | Chagos | Composite (GIM, PIE, COI5) | 1881-1995 (115) | 0.02 | 0.09 | +0.26 | **0.34** | **<0.00** | **+0.61** | **0.29** | **<0.00** | **+0.54** |
| | Kenya | Mal 96-1 | *No monthly data available* | | | | | | | | | |
| | Tanzania | Mafia | 1897-1995 (99) | **0.29** | **<0.00** | **+1.03** | **0.39** | **<0.00** | **+0.73** | **0.50** | **<0.00** | **+0.68** |
| | **Average** | | | | | +0.95 | | | +0.74 | | | +0.58 |
| **Subtropical** | Mayotte | AND3 | 1882-1995 (114) (to 1993 for coral record) | **0.25** | **<0.00** | **+0.87** | 0.10 | **<0.00** | +0.34 | **0.35** | **<0.00** | **+0.52** |
| | Madagascar (NE region) | Big Mum | 1952-1995 (44) | 0.05 | 0.15 | +0.39 | **0.47** | **<0.00** | **+0.86** | **0.17** | **<0.00** | **+0.40** |
| | Madagascar (Antongil Bay) | MAS1 | 1966-1995 (30) | 0.08 | 0.12 | -0.62 | 0.15 | 0.04 | +0.39 | 0.01 | 0.61 | +0.10 |
| | Madagascar (St. Marie Is) | STM2 | 1956-1995 (40) | **0.31** | **<0.00** | **+1.40** | **0.44** | **<0.00** | **+0.78** | 0.12 | 0.03 | +0.33 |
| | Madagascar (SW region) | Ifaty-4 | 1870-1995 (126) | **0.08** | **<0.00** | **-0.63** | 0.00 | 0.49 | +0.07 | **0.18** | **<0.00** | **+0.54** |
| | Reunion Is. | Composite (LaRe-1, LaRe-Jens, St. Rose) | 1913-1995 (83) | **0.15** | **<0.00** | **+0.77** | **0.31** | **<0.00** | **+0.64** | **0.20** | **<0.00** | **+0.52** |
| | Rodrigues Is. | Composite (Totor, Cabri) | 1870-1995 (126) | **0.21** | **<0.00** | **+1.14** | **0.09** | **<0.00** | **+0.38** | **0.16** | **<0.00** | **+0.47** |
| | **Average** | | | | | +0.47 | | | +0.49 | | | +0.41 |

Values in bold are significant at 5% level

### *3.4. Wavelet analysis*

The time series of the SST anomaly for the Seychelles-Chagos combination is shown in Figure 3.12(a). The wavelet power spectrum for the Seychelles-Chagos combination was done for the period 1841-2002 (Figure 3.12(b)) from 3 cores (NEP, BVB, SA) from Seychelles and 3 cores (GIM, PIE, COI5) from Chagos.

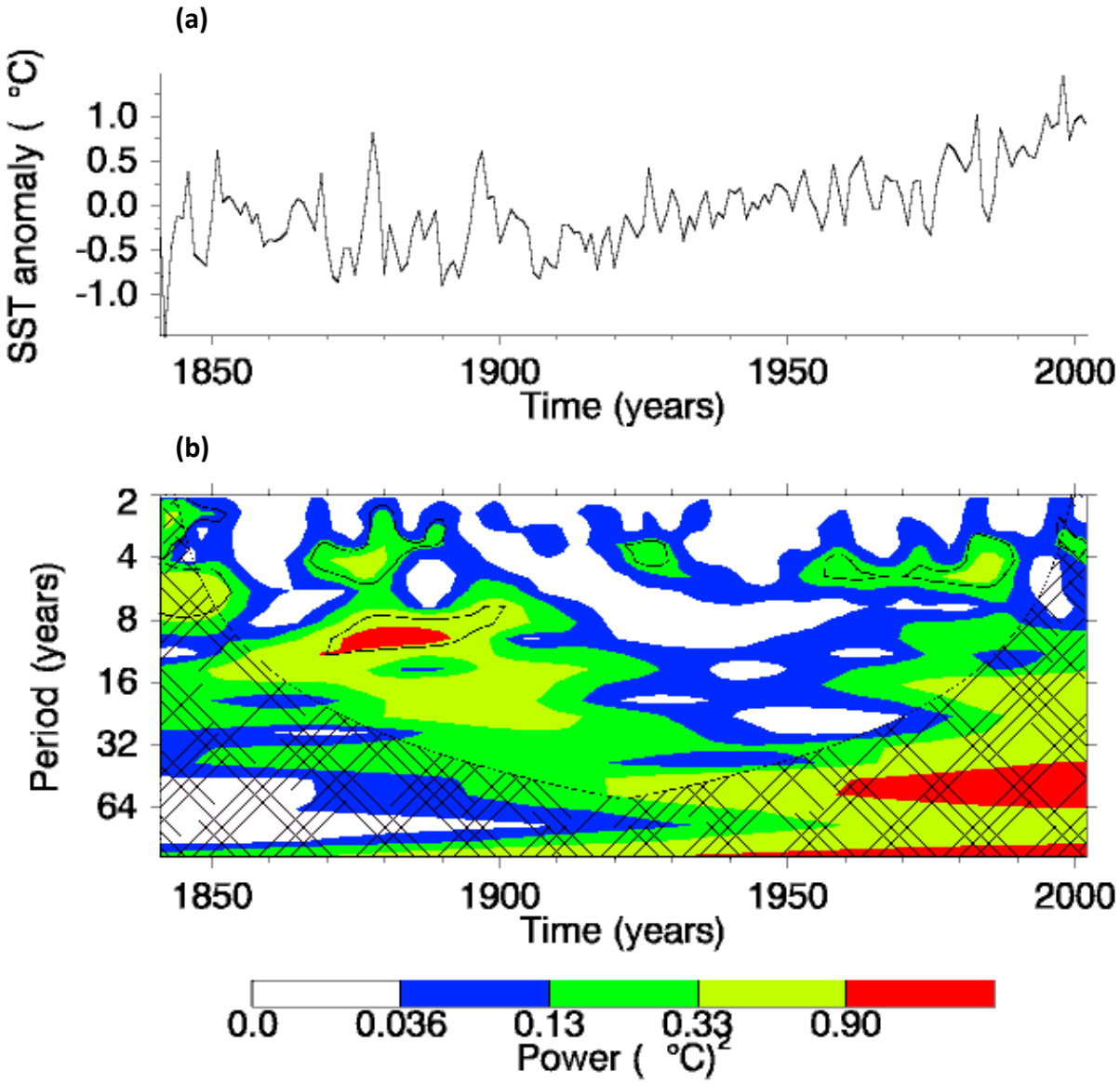


**Figure 3.12. (a) Annual time series of the Seychelles-Chagos combination SST anomaly from 6 cores from 1841 to 2002. (b) Wavelet power spectrum computed with the method of Torrence and Compo (1998), where black contours show the amplitude within which confidence level is 90% against a red noise background. Cone of influence is delineated by the stippled line, where variance has been reduced with zero padding.**

Interannual and decadal variability is predominantly observed for the Seychelles-Chagos combination (Figure 3.12(b)), with strong variability before 1890 and after 1950. The decadal variability falls outside the cone of influence before 1850 and after 2000. Significant variability (at the 90% level) is roughly centered at periods 3-6 years and 10-12 years.

For Kenya, the time series of the SST anomaly is shown in Figure 3.13(a) and the wavelet power spectrum is performed for the period 1801-1994 (Figure 3.13(b)) from the coral $\delta^{18}O$ data from the core Mal96-1. The wavelet analysis shows significant interannual variability (at the 90% level) centered approximately at periods 3-5 years. It should be noted that interdecadal variability is observed as from 1940 with periods about 48 years ,but falls outside the cone of influence.

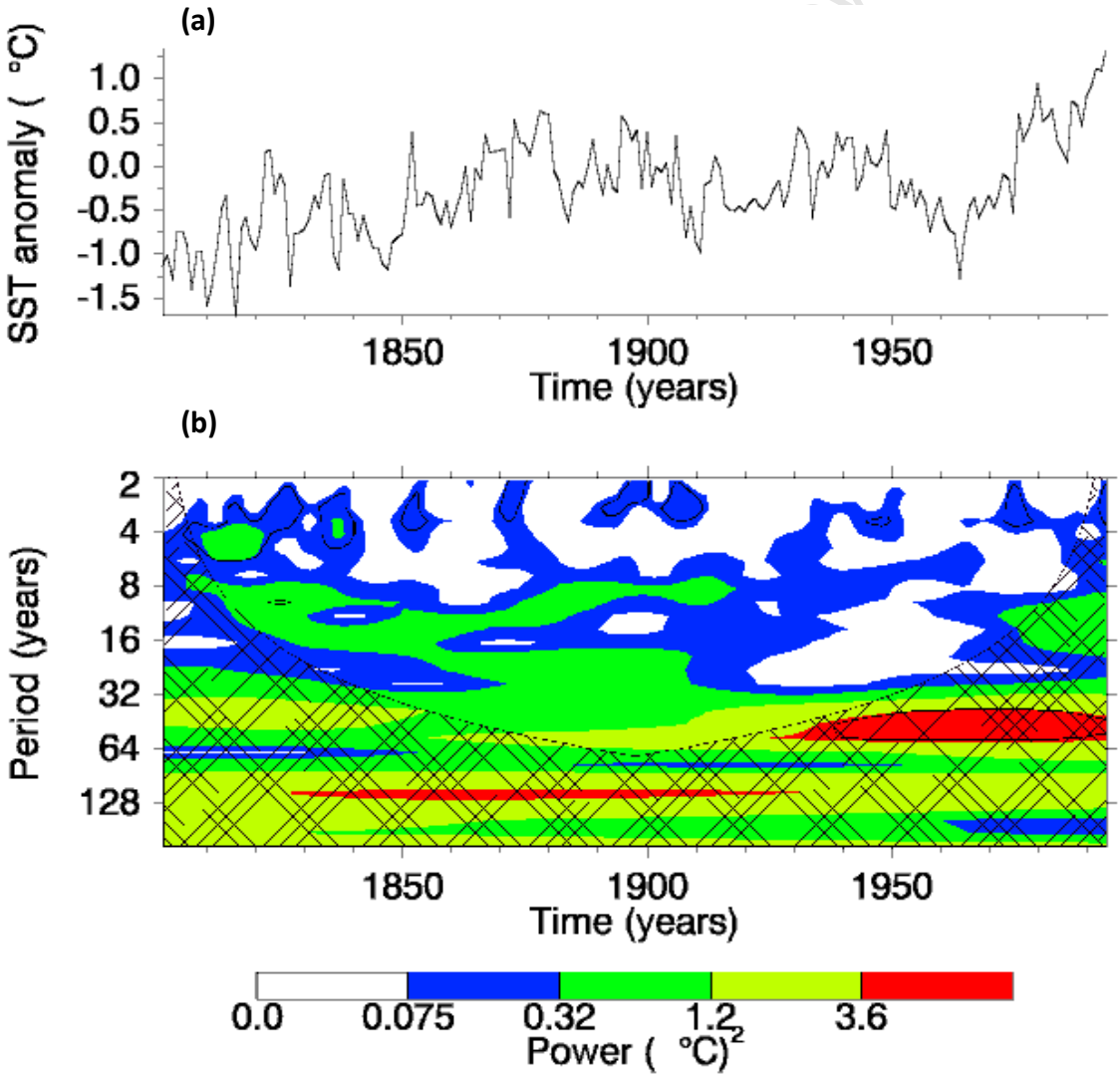


**Figure 3.13. (a) Annual time series of Kenya SST anomaly from 1801 to 1994. (b) Wavelet power spectrum computed with the method of Torrence and Compo (1998), where black contours show the amplitude within which confidence level is 90% against a red noise background. Cone of influence is delineated by the stippled line, where variance has been reduced with zero padding.**

The time series of the SST anomaly derived from coral $\delta^{18}O$ data, obtained from the core Mafia is computed from 1897 to 1997 for Tanzania (Figure 3.14(a)). The wavelet power spectrum is done for the same period (Figure 3.14(b)). Significant interannual variability (at the 90% level) is roughly situated at periods 3-6 years.

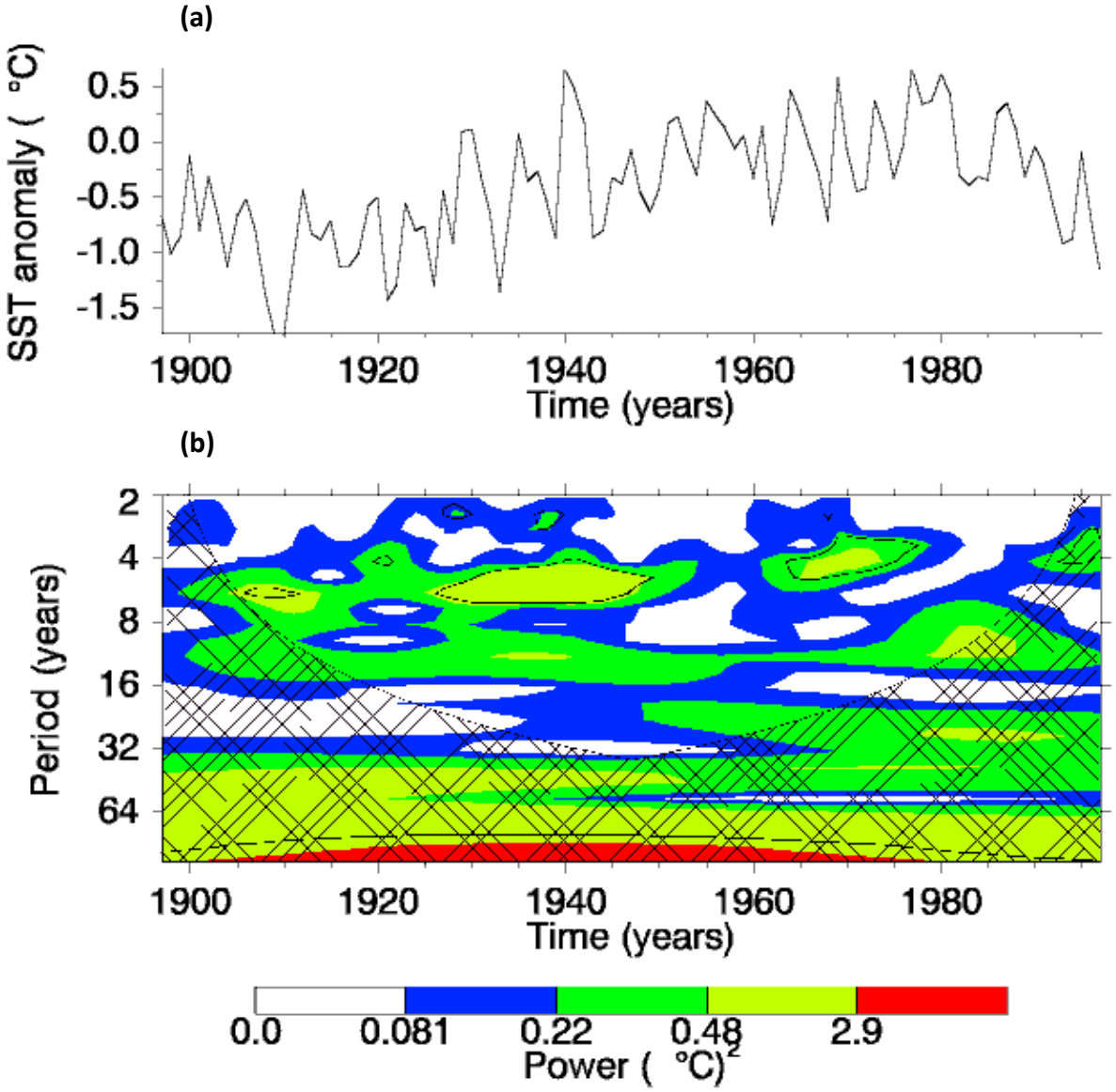


**Figure 3.14. (a) Annual time series of Tanzania SST anomaly from 1897 to 1997. (b) Wavelet power spectrum computed with the method of Torrence and Compo (1998), where black contours show the amplitude within which confidence level is 90% against a red noise background. Cone of influence is delineated by the stippled line, where variance has been reduced with zero padding.**

The period 1882-1993 is used to compute the time series of the SST anomaly from the composite core AND3 ($\delta^{18}O$ and Sr/Ca data) (Figure 3.15(a)) and the wavelet power spectrum (Figure 3.15(b)) for Mayotte. The wavelet analysis indicates significant interannual variability (at the 90% level) after 1925 with periods around 3-6 years.

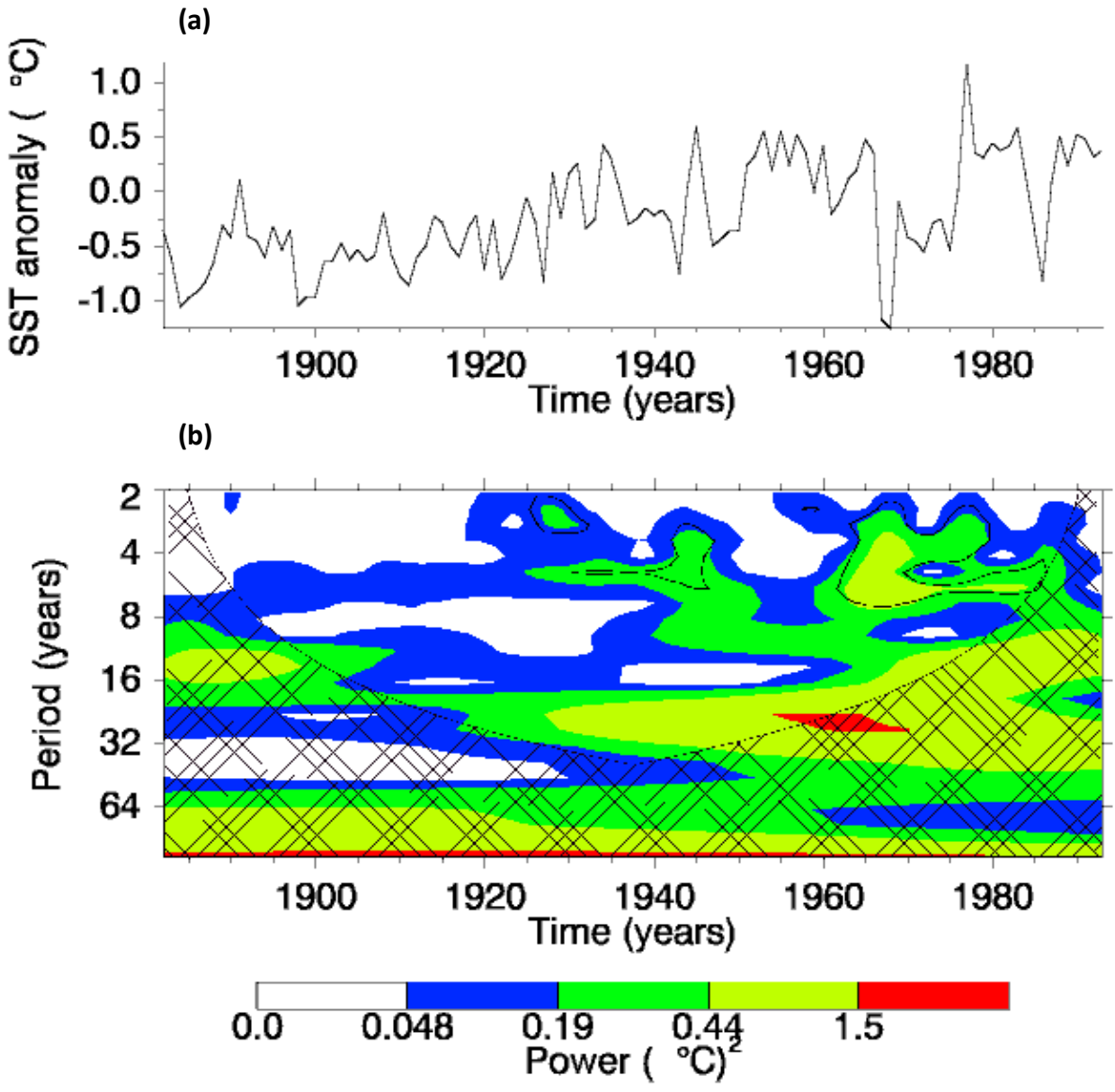


**Figure 3.15. (a) Annual time series of Mayotte SST anomaly from 1882 to 1993. (b) Wavelet power spectrum computed with the method of Torrence and Compo (1998), where black contours show the amplitude within which confidence level is 90% against a red noise background. Cone of influence is delineated by the stippled line, where variance has been reduced with zero padding.**

For the south-western region of Madagascar, the time series of the SST anomaly (Figure 3.16(a)) and the wavelet power spectrum (Figure 3.16(b)) are performed for the period 1660-1994 with $\delta^{18}O$ proxy data from 3 cores (Ifaty-1, Ifaty-4 and Tulear-3). The wavelet analysis reveals significant interannual variability (at the 90% level) with periods centered approximately at 3-7 years. Decadal variability is also observed with a period of about 15 years in the early 18$^{th}$ century and mid-19$^{th}$ century. Quasi-centennial variability with a periods centered around 96-128 years occurs until 1970. However, most of this signal falls outside the cone of influence, except for the period 1810-1890.

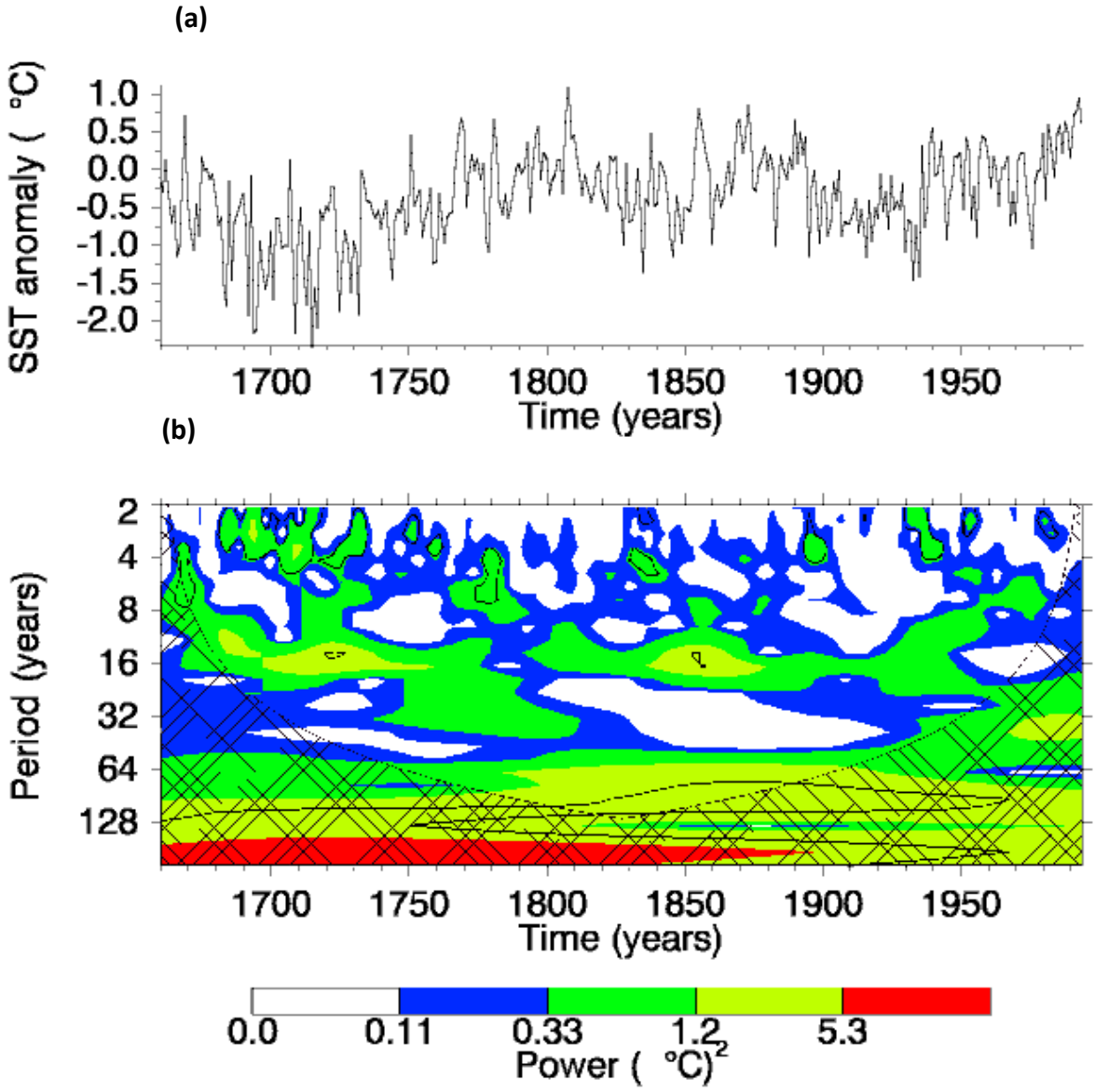


**Figure 3.16. (a) Annual time series of Madagascar (south-western region) SST anomaly from 1660 to 1994. (b) Wavelet power spectrum computed with the method of Torrence and Compo (1998), where black contours show the amplitude within which confidence level is 90% against a red noise background. Cone of influence is delineated by the stippled line, where variance has been reduced with zero padding.**

The time-series for Rodrigues Island is given in Figure 3.17(a) and the wavelet power spectrum is shown in Figure 3.17(b) from 1781 to 2005. Significant variability is centered (at the 90% level) roughly at periods 2-4, 8-10 and 20 years. Lower frequency variability at around 60-128 years is located outside the cone of influence.

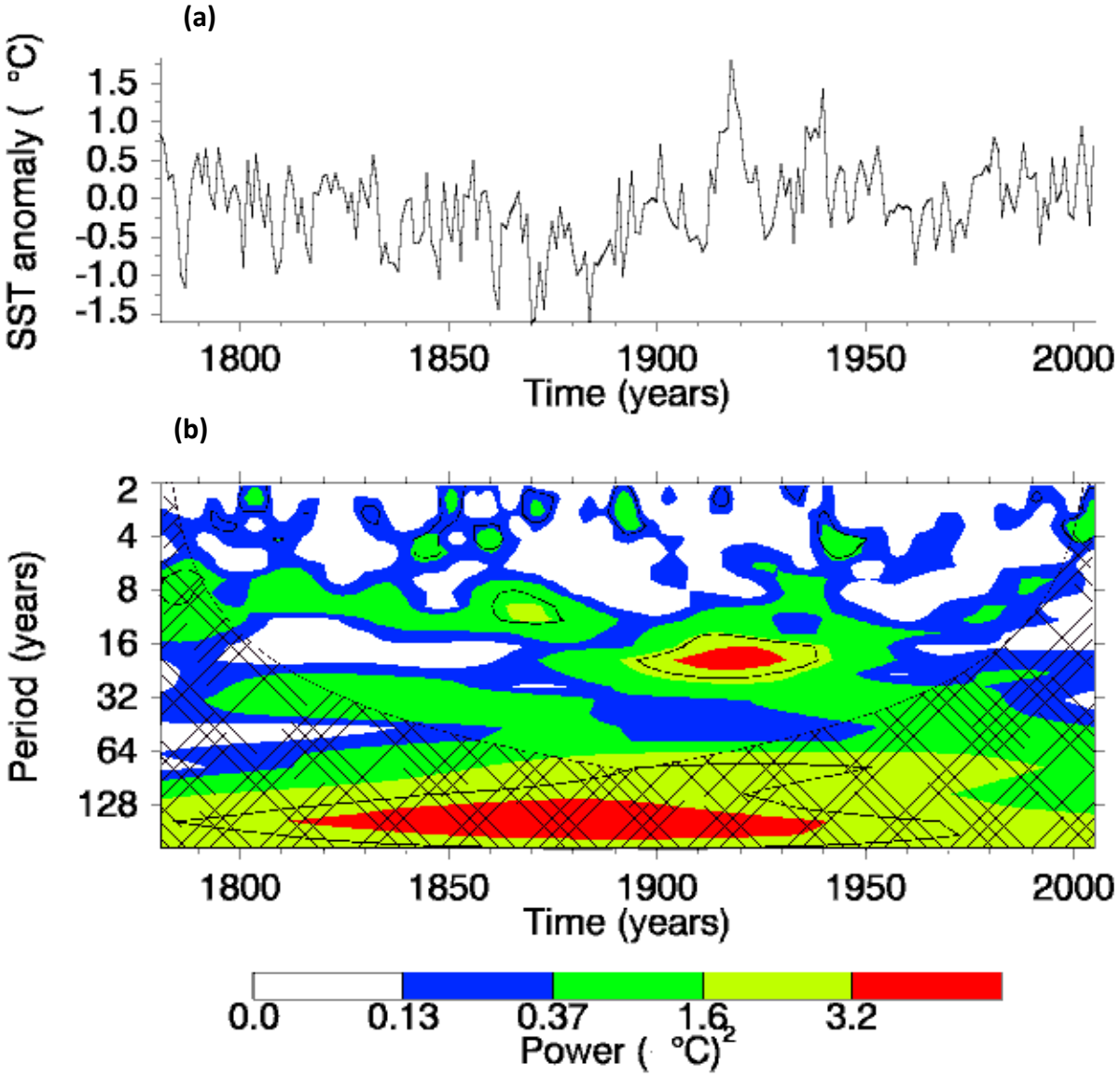


**Figure 3.17. (a) Annual time series of Rodrigues Island SST anomaly from 1781 to 11994. (b) Wavelet power spectrum computed with the method of Torrence and Compo (1998), where black contours show the amplitude within which confidence level is 90% against a red noise background. Cone of influence is delineated by the stippled line, where variance has been reduced with zero padding.**

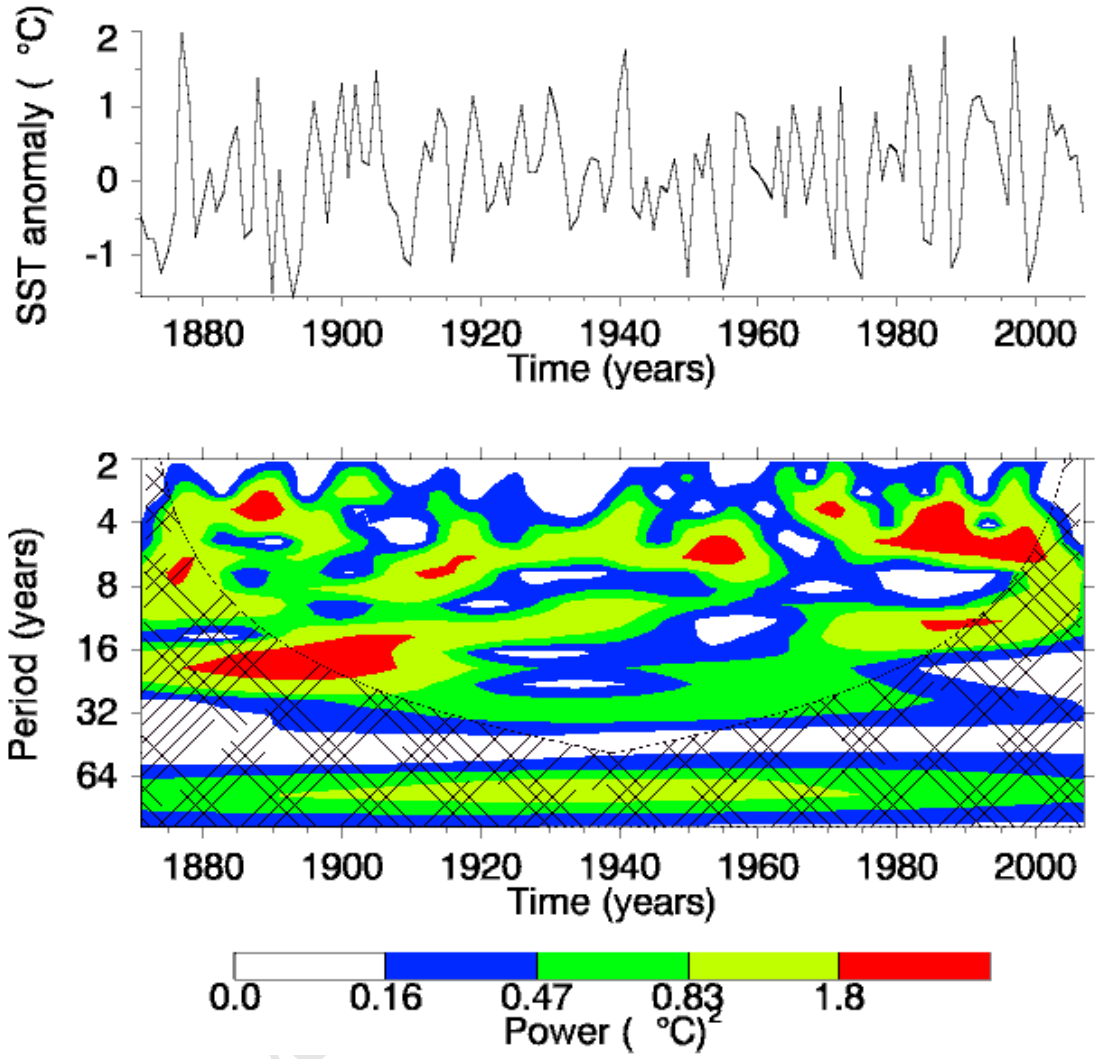


**Figure 3.18. (a) The Niño3.4 SST index time series from 1871 to 2007. (b) Wavelet power spectrum computed with the method of Torrence and Compo (1998). Cone of influence is delineated by the stippled line, where variance has been reduced with zero padding.**

The time-series for the Niño3.4 SST index is given in Figure 3.18(a) and the wavelet power spectrum is shown in Figure 3.18(b) from 1871 to 2007. The Niño3.4 SST index data are downloaded from the Climate and Global Dynamic's (CGD) climate analysis section website available at *http://www.cgd.ucar.edu/cas/catalog/climind/TNI_N34/index.html#Sec5*. It is evident that highest power (shown in red and yellow) are centered around 3-7 years on interannual time scales. The

interdecadal variability centered around 12-24 years are also observed, especially in the first few decades and around 1980.

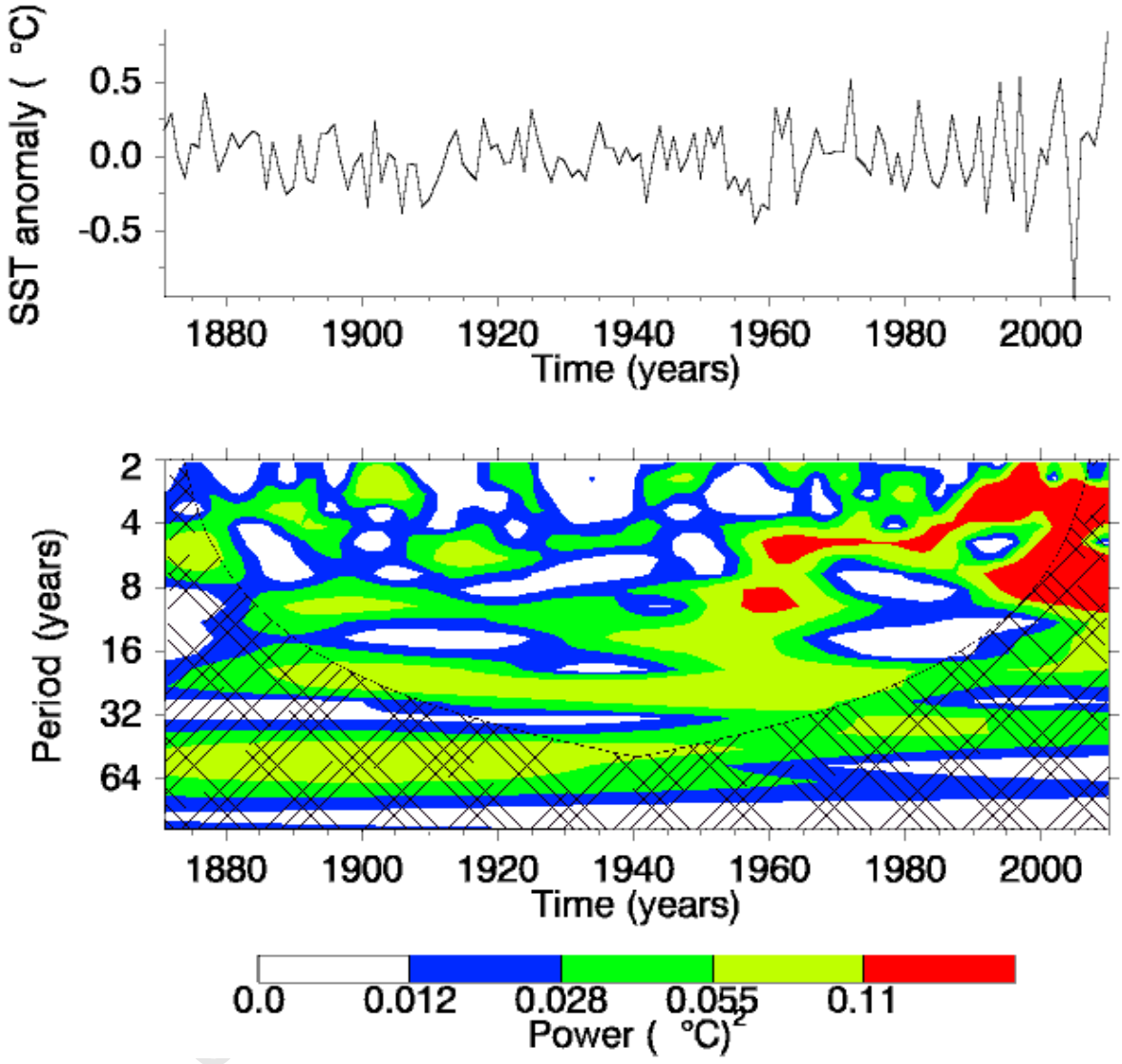


**Figure 3.19. (a) The SST DMI time series from 1871 to 2010. (b) Wavelet power spectrum computed with the method of Torrence and Compo (1998). Cone of influence is delineated by the stippled line, where variance has been reduced with zero padding.**

The SST DMI time series is given in Figure 3.19(a) and the wavelet power spectrum is shown in Figure 3.19(b) from 1871 to 2010. The SST DMI data is derived from the HadISST dataset and is downloaded from *http://www.jamstec.go.jp/frsgc/research/d1/iod/e/iod/dipole_mode_index.html*. High power (shown in red and yellow) are roughly centered at periods 3-6 and 9 years. Highest power are observed after 1955 and is centered around 5 and 9 years.

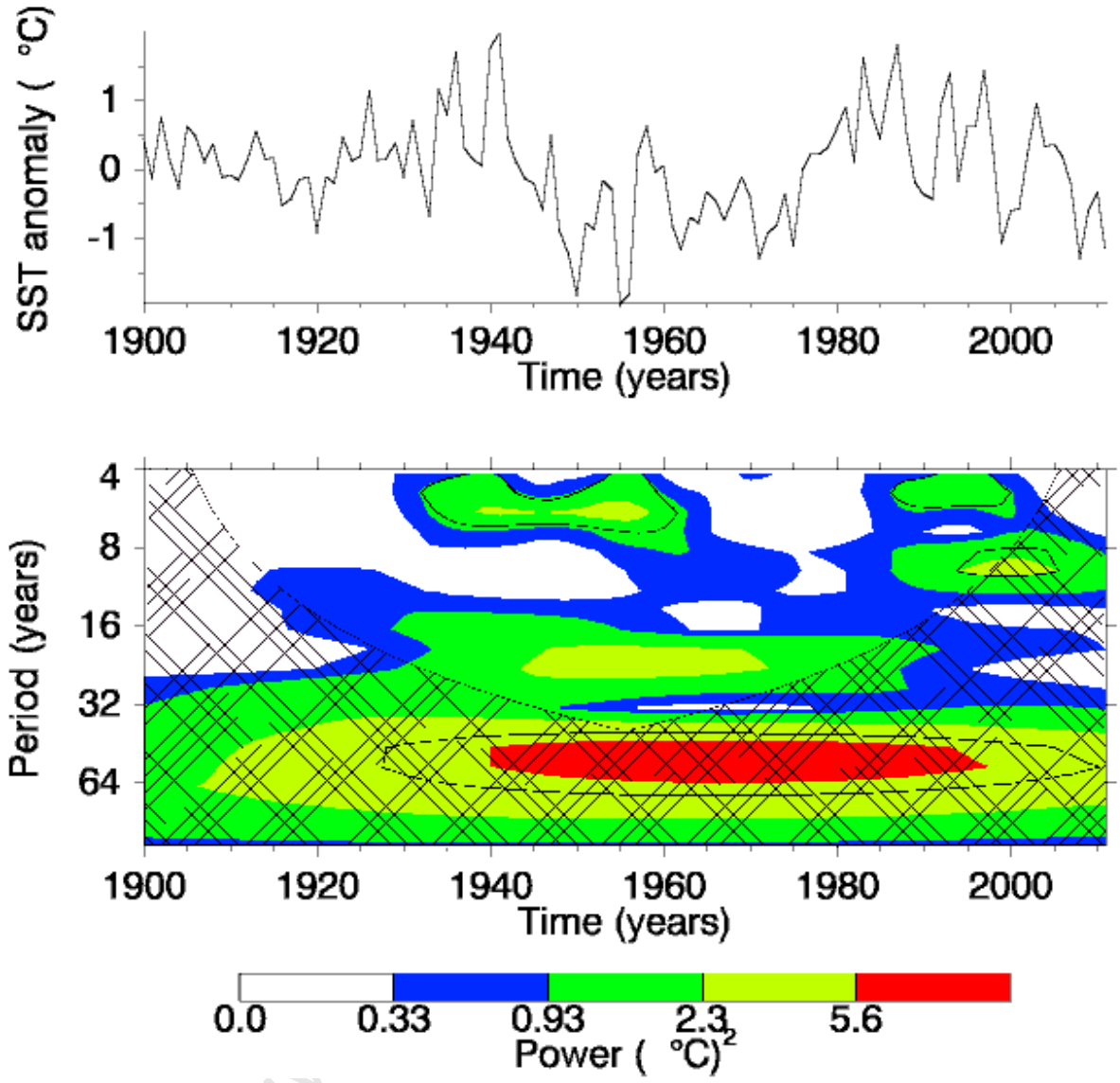


**Figure 3.20. (a) The PDO index time series from 1900 to 2011. (b) Wavelet power spectrum computed with the method of Torrence and Compo (1998), where black contours show the amplitude within which significance level is 90% against a red noise background. Cone of influence is delineated by the stippled line, where variance has been reduced with zero padding.**

The PDO index time series is given in Figure 3.20(a) and the wavelet power spectrum is shown in Figure 3.20(b) from 1900 to 2011. The PDO index data are downloaded from *http://jisao.washington.edu/pdo/PDO.latest*. Highest variability is noted approximately at periods 18-26 years (in yellow) and 48-64 years (in red). Interannual variability is not taken into consideration from the wavelet power spectrum above.

# 4.0. Discussion

## *4.1. Correlation of coral records with satellite sea surface temperature (SST) data*

Investigating the relationship between the coral proxy data and AVHRR SST showed a relatively high correlation coefficient on monthly time scales owing to the presence of substantial seasonality; thus, there is a certain degree of autocorrelation. On the other hand, lower correlation coefficient values are observed for the annual mean data. The latter situation is due to the fact that the seasonal cycle is lost when linear annual averages are considered. While analysing the results of correlation between Sr/Ca and SST from literature, Scott et al. (2010) found that the relationship is much higher on seasonal time scales, whereas weaker but significant correlation was predominantly observed for data when seasonality was removed. A greater variance in SST on seasonal time scales, the match-up of seasonal extremes of measured geochemical proxies to extremes of SST for creation of monthly chronology may potentially explain the higher correlations when dealing with the seasonal cycles (Scott et al., 2010). These higher correlation values on seasonal time scales may also be explained by unknown factors making isotopes and influencing chemicals absorbed in coral skeletons. The latter could be linked to strong seasonality factors in the environment (sunlight, nutrients concentration, growth rate, etc) (Scott et al., 2010). In addition, the extent to which geochemical proxies, particularly Sr/Ca, are sensitive to SST can vary as much within coral genus as between species (Scott et al., 2010). When coral records taken from the same coral species and from the same location a few kilometres apart are correlated with the same grid point of AVHRR SST, in some cases, slightly different correlation coefficients are observed on monthly and annual time scales, as seen for instance, with the records MAS1, ANDRA, IFAHO from Antongil Bay, Madagascar. This result could be due to non-SST factors and local oceanic conditions that drive chemical and isotope absorption into the coral skeletons (Scott et al., 2010).

## *4.2. Degree Heating Month*

DHM is a technique used to predict coral thermal stress in response to positive SST anomalies and subsequent coral bleaching (McClanahan et al., 2007). The higher the DHM value for a particular year, the higher is the probability for coral bleaching to occur during the summer period of this year. Most studies using DHM to assess coral thermal stress calculated DHM from long-term instrumental and satellite SST data sets such as HadISST and ERSSTv2 (Carilli et al., 2010) and GISST 2.2 and IGOSS-NMC (Lough, 2000). Predicting coral thermal stress from coral proxy data has not been performed before. Stress bands have been used to examine the history of coral bleaching (Carilli et al., 2010).

In general, nearly the same trends in DHM are observed when comparing the results from the coral SST, ERSSTv3 and HadSST1.1 data for the sites investigated (Figures 3.1-3.11). Even though the coral DHM aligns quite well with instrumental DHM, the maximum annual accumulated thermal stress calculated from coral data generally showed a higher DHM value as compared to that from ERSSTv3 and HadSST1.1. For most of the sites analysed in the WIO, the maximum DHM determined from coral data is generally about 2-3 times greater than the maximum DHM calculated from the two instrumental datasets. Although this difference is in magnitude, it is obvious than there is an increase in DHM values for the tropical and subtropical sites in the WIO and there is no evident difference in the occurrence rate of DHM in the tropics and the subtropics.

Since the end of the 1970s, a rise in the occurrence of mass coral bleaching episodes has been observed (Lough, 2000). In fact, the results suggested that DHM values have increased from the 1970s until very recently. Instrumental data generally agree with the coral data regarding this increase, although the magnitude of the DHM derived from coral data is bigger. Many coral reefs across the globe experienced an unprecedented massive bleaching in summer 1998 (Lough, 2000; Wilkinson, 2000; Smith et al., 2008b) principally owing to high SST associated with the very strong El Niño and the Indian Ocean Dipole of that year. Most Indian Ocean reefs also suffered during this year and more than 90% of shallow corals died (Sheppard, 2003). Following the 1998 episode, bleaching events may become more and more common with global warming as the thermal tolerances of corals are surpassed each year within the next few decades (Hoegh-Guldberg, 1999).

The combined Seychelles-Chagos record is representative of the tropical WIO region. The year 1998 during which very strong El Niño and IOD events occurred (Hong et al., 2008) recorded the highest thermal stress for the Seychelles-Chagos combination for proxy and instrumental SSTs during the period analysed (Figure 3.3). The maximum DHM value recorded for the coral SST is nearly thrice that for ERSSTv3 and about twice that for HadSST1.1. The highest annual accumulated thermal stress was noted with ERSSTv3 and HadSST1.1 data in 1998 for some tropical sites like Seychelles and the Seychelles-Chagos combination. The years following 1998 further recorded maximum DHM values such as in 2003 with coral SST for Seychelles, 2002 with coral SST for Reunion Island and 2007 with ERSSTv3 for Ifaty (Madagascar). However, most of the subtropical sites under investigation in the WIO such as Ifaty and St. Marie Island in Madagascar, Rodrigues Island and Reunion Island did not record very high DHM values in 1998. Local atmospheric and oceanic conditions, such as high cloud cover and rainfall, or surface cooling due to winds, that were prevailing at these sites during this particular time may explain the moderate DHM values noted (Obura, 2005; McClanahan et al., 2007).

Most of the sites in both the tropical and subtropical WIO show that high DHM values coincide with these ENSO events and sometimes in conjunction with positive IOD events. For instance, high DHM values occurred in the Seychelles-Chagos combination during all the above ENSO years from 1841 onwards, except in 1891. Moreover, the subtropical site, Rodrigues Island has also recorded high occurrence of DHM during the ENSO years, except in 1828 and 1957-1958 when strong DHM values were not that evident.

Regions in the WIO with historically higher SST variability experienced less coral mortality after the 1997-1998 ENSO event (McClanahan et al., 2007; Ateweberhan and McClanahan, 2010). In fact, the occurrence of coral bleaching is principally determined by the history of past SST variability , where corals experiencing high SST variability possess a higher bleaching threshold and resist bleaching, while corals with low SST variability may not survive a moderate SST rise (Donner, 2011). Many sites in the WIO possess a long history of high DHM and they might be better adapted to survive increase in SST. Chagos and the Seychelles-Chagos combination are sites from the tropics with historically higher SST variability. Seychelles recorded a low to moderate DHM. In the subtropics, Reunion Island, St. Marie Island and Antongil Bay from Madagascar experienced low to moderate DHM in the past. Moderate to high DHM values were recorded in Rodrigues Island and in the south-western region of Madagascar. On the other hand, sites that did not record high DHM in the past are the north-eastern region of Madagascar, Mayotte and Tanzania. The latter three sites possessing historically lower DHM might be less prepared to survive future warming, unless they experience low warming rates in the future. Seychelles (low-moderate DHM in the past) was among the sites whose reefs were most severely affected in the 1997-1998 ENSO event, whereas Reunion Island, Rodrigues Island, Madagascar and Mayotte reefs' were the least affected after 1998 (Ateweberhan and McClanahan, 2010), most probably due to their historical low to moderate DHM and/or local oceanic conditions mitigating rises in SST.

In addition, it is worthwhile to point out that the DHM measure alone might not be a good predictor for coral bleaching events in some cases (Carilli et al., 2010). Local anthropogenic stressors such as increased sedimentation due to deforestation on land or dredging in the sea might reduce coral thermal tolerance and cause bleaching, even during a moderate warming event (Carilli et al., 2010). A higher DHM value that occurs without no major added anthropogenic stressors might not lead to bleaching and death of the coral if it can survive and recover. On the other hand, a moderate DHM value, that is a medium thermal stress, occurring at the same time as increased local stresses can cause the coral to bleach and die due to its reduced thermal tolerance (Carilli et al., 2010). Therefore, sites with a long history of high DHM and not affected by additional anthropogenic stressors can be

said to be relatively resilient to warm SST anomalies and bleaching and consequently act as sanctuaries for the maintenance of coral reefs biodiversity (West and Salm, 2003).

Future analysis should consist of re-working the DHM values for the coral SST by considering the error based on the slope of uncertainties of proxy versus SST. The DHM values of coral SST which were higher in magnitude than the instrumental SSTs could be reduced by taking into consideration the slope of uncertainties when converting coral proxy data into coral SST. The geochemical proxy Sr/Ca from corals have not been unanimously accepted in reconstructing past SST because coral Sr/Ca records during the last deglaciation and early Holocene reveal a larger decrease in tropical Indo-Pacific SST (~3-6 $^{o}$C) (e.g., DeLong et al., 2010) compared to a tropical cooling of only ~2-4 $^{o}$C recorded from Mg/Ca in planktonic foraminifera during the Last Glacial Maximum (e.g., Linsley et al., 2010).

Gagan et al. (2012) examined the possibility that coral paleotemperature overestimate changes in SST on decadal to millennial time scales. In fact, records from corals are weakened during the process of skeletal formation within the living tissue layer and therefore, calibrations with reduced sensitivities for *Porites* are needed in order to reconstruct seasonal to interannual changes in SST more accurately (Gagan et al., 2012). For $\delta^{18}$O-SST sensitivities the value of -0.23 ‰ $^{o}C^{-1}$ (as compared to the mean value of -0.20 ‰ $^{o}C^{-1}$ used in this study) should be used and for Sr/Ca-SST sensitivities, the rescaled value of -0.084 mmol/mol $^{o}C^{-1}$ (as compared to the mean value of -0.06 mmol/mol $^{o}C^{-1}$ used in this study) should be utilised to calculate SST trends for the 20$^{th}$-century and changes in mean SST on millennial time scales (Gagan et al., 2012).

### *4.3. Warming trends*

This section of the thesis showed clearly that in general, both the tropical and subtropical WIO have been warming during the period 1870-1995, but with different and varying rates as recorded by coral SST and instrumental SSTs. Globally, there has been a rise in mean SSTs of 0.4-0.8 °C during the last century (McCarthy et al., 2001). The analysis of long coral data from Seychelles, Kenya, Madagascar and Western Australia reveals a rise in SST about 0.8-1.4 °C during about the last two centuries, but with more pronounced warming since the 1970's (Cole et al., 2000; Zinke et al., 2004, 2005). These findings are more or less consistent with the increase in SST recorded from coral data used in this study (Table 3.2), with an increase of 0.8 °C for the tropical WIO and 0.5 °C for the subtropical WIO for the period 1870-1995.

It is not possible to state with certainty that the tropical region has been warming more than the subtropical region in the WIO throughout the full period considered in this thesis because statistical

analysis showed that this was evident only with the instrumental SSTs and not in the coral data. The seasonal trends also suggested that, on the whole, both the tropical and subtropical WIO warmed during summer as well as in winter, yet with different rates as indicated with coral and instrumental SSTs. Warming is higher for some sites with coral SST but there are weaker warming trends for other sites with instrumental SSTs, and vice versa.

Cooling was observed near the south-western region of Madagascar with coral SST (Ifaty-4 cores) (but not with the instrumental SSTs) for the annual trend analysis and for the seasonal trends, although the latter were not significant for summer. However, by using a composite coral record consisting of 3 cores (Ifaty-1, Ifaty-4 and Tulear-3) from the south-western region of Madagascar during the 1870-1995 period, a warming trend of +0.33 $^{o}$C ($R^2$= 0.33, p=0.04, not shown in Table 3.3) is observed. During the same period, a warming trend of +0.50 $^{o}$C was observed with HadSST1.1 in the south-western region (Table 3.2). This warming is consistent with the findings of McClanahan et al. (2009) who found that the south-western reefs of Madagascar have experienced a fast temperature rise of ~0.88 $^{o}$C during the past 5 decades. Therefore the Ifaty-4 record alone may not be appropriate to calculate the trends, and a possible reason could be that the Ifaty-4 corals may have been growing under stressed conditions and the tracers in the skeletons may not be really related to SST (Zinke, personal communication). The north-eastern region of Madagascar also indicated cooling with coral SST for the winter trend, but this was not significant.

It was noticeable that the sites from Madagascar had relatively lower warming rates compared to other sites. This could be explained by the local oceanic settings prevailing at these sites favouring moderate to low warming of the water and therefore acting as potential thermal refuges for coral reefs, hence increasing their survivorship in respect to predicted future warming. For instance, McClanahan et al. (2009) reported that eastern reefs of Madagascar (including Antongil Bay and St. Marie Island regions) had lower temperature increases compared to the south-western reefs. In addition, these reefs possess a well consolidated structure that could potentially be more prepared to survive global change (McClanahan et al., 2009). On the other hand, the sites with higher warming rates like Seychelles and Chagos from the tropical WIO as showed by coral SST and instrumental SSTs, suggested that they might not offer the appropriate conditions for the survival of coral reefs for the future unless if they possess naturally high SST variability.

The coral proxy-SST sensitivities could affect the magnitude of long-term warming trends from *Porites* coral data. Coral paleotemperature could overestimate changes in SST on long-term time scales (Gagan et al., 2012). In this study, warming trends, like DHM were calculated using the value

of -0.23 ‰ $^{o}C^{-1}$ for $\delta^{18}O$-SST sensitivities and -0.06 mmol/mol $^{o}C^{-1}$ for Sr/Ca-SST sensitivities. The magnitude of the warming trends from coral data in the WIO could therefore be different by using the values (-0.23 ‰ $^{o}C^{-1}$ for $\delta^{18}O$-SST and -0.084 mmol/mol $^{o}C^{-1}$ for Sr/Ca-SST) proposed by Gagan et al. (2012).

### *4.4. Wavelet analysis*

In general, all the coral data from both the tropical and subtropical sites show on average similar interannual variability with periods centered around 3-6 years. Nearly all of these interannual modes are statistically significant (at 90% level). This is more or less consistent with the findings of Ashok et al. (2003) who reported that the tropical Indian Ocean region has significant variability with a peak scale of about 3.6 years. Significant decadal variability (at 90% level) is observed for Seychelles-Chagos combination in the tropics, and Madagascar (south-western region) and Rodrigues Island in the subtropics. The decadal modes vary from periods of 10 to 20 years. It should be noted that the interannual and decadal variability do not persist through time. The signals at interdecadal and longer time scales were not statistically significant (at 90% level), since most of them fall outside the cone of influence in the wavelet analyses.

Wavelet power spectra were also generated for the Niño3.4 SST index (Figure 3.18(b)) with evident interannual variability at periods 3-7 years, the SST DMI (Figure 3.19(b)) with highest variability at periods 3-6 and 9 years and the PDO index (Figure 3.20 (b)) with highest variability at periods 18-26 years and 48-64 years. In most literature, it is noted that the periodicities of ENSO are roughly around 3-7 years (Ashok et al., 2003; Crueger et al., 2009; MacMynowski and Tziperman, 2008). Therefore, the 3-6 year period in the coral data for most of the WIO sites suggests an ENSO influence. Concerning the periodicities for the IOD index, Ashok et al. (2003) reported that it is significantly centered around 5.2 years, which is in the range of the periods (3-6 years) observed in Figure 3.19(b) for the SST DMI. The periodicities for the PDO have been from 15-25 years and from 50-70 years during the last 100 years (Mantua and Hare, 2002). Periods centered around 50 years and around 96-128 years were observed for the coral data from Kenya and Rodrigues Island respectively. It is not clear whether these signals are related to the PDO or to some other slower mode.

Future work could consist of performing cross-wavelet coherence in order to confirm whether the periods in each coral data is really related to one of the suggested climate indices or not.

## 5.0. Conclusion

The coral records from the WIO are found to correlate significantly with AVHRR SST on monthly time scales and higher correlation values are obtained on monthly or bimonthly time scales compared to annual time scales. The prediction and comparison of coral thermal stress by the DHM technique from coral and instrumental SSTs reveals that coral DHM aligns quite well with instrumental DHM, yet the DHM values from coral data are generally 2-3 times greater in magnitude than the DHM values from the two sets of instrumental data. Also, the results showed that the annual accumulated thermal stress for most tropical and subtropical sites seems to be increasing since the 1970's, which is consistent with the rise in the occurrence of mass coral bleaching events since the end of the 1970's as reported by authors such as Lough (2000). The establishment of the heterogeneous distribution of warming rates from 1870 to 1995 indicates that in general, both the tropical and subtropical sites have been warming, but with different and varying rates as recorded by the coral and the two instrumental SST datasets at the various WIO sites investigated. In fact, varying trends were also observed within the seasons and it was evident that both the tropical and the subtropical WIO warmed during both summer and winter periods from 1870 to 1995. The analysis of the coral records on longer time scales revealed that significant interannual variability was approximately centered at periods 3-6 years, which is most probably linked to ENSO and IOD signals. An attempt made to classify the sites where coral reefs are better geared to survive climate change based on historical SST variability and intensity of warming rates suggests that corals in the WIO are located in different oceanographic conditions and some corals may be more favoured to survive warming climate compared to others. Coral reefs from sites such as Seychelles and Chagos which experienced mostly high SST variability and generally high warming rates should in fact be better prepared to survive climate change as long as they can cope with increasing SSTs and their bleaching threshold is not surpassed. Coral reefs located at St. Marie, Antongil Bay (Madagascar) and from Reunion Island with historically low to moderate SST variability and experiencing moderate to high warming rates might suffer with respect to future warming. Concerning corals located in south-western Madagascar and in Rodrigues Island, it was found that they have historically moderate to high SST variability and experience moderate to high warming rates. Therefore, they might be better able to survive climate change. Coral reefs at sites with little or no history of high SST variability such as north-eastern Madagascar, Mayotte and Tanzania which experience low warming rates might be better prepared to survive global change if warming does not increase dramatically in the future.

## 6.0. Appendix

### *6.1. Correlation of coral records with satellite SST data*- Example of regression graph

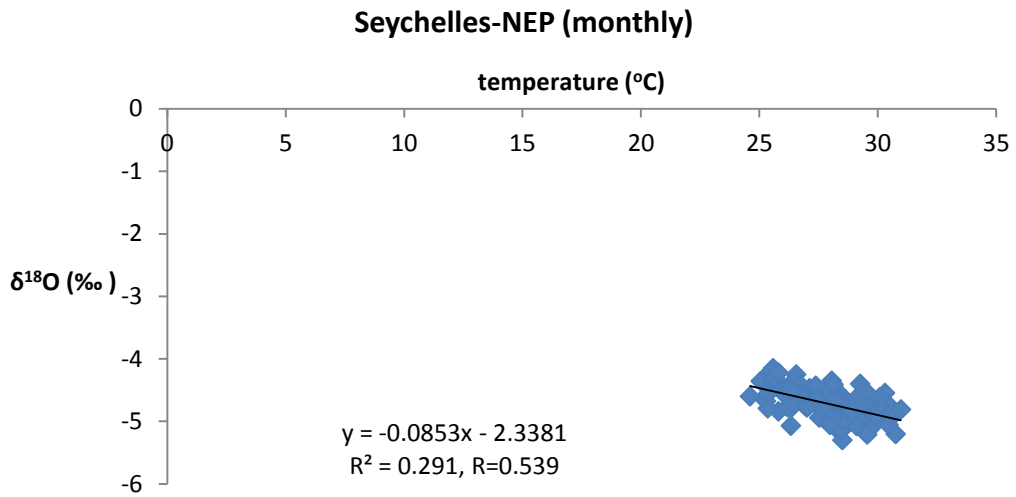


**Figure 6.1. Graph showing the correlation of coral records with satellite SST data for Seychelles (NEP) on monthly time scales**

**Table 6.1. Coefficients, Standard Error, t-stat, p-value, lower and upper limit of 95% C.I for regression in Figure 6.1.**

| | *Coefficients* | *Standard Error* | *t Stat* | *P-value* | *Lower 95.0%* | *Upper 95.0%* |
|---|---|---|---|---|---|---|
| Intercept | -2.3380935 | 0.314624386 | -7.431380411 | 9.20685E-12 | -2.960046435 | -1.716140564 |
| X Variable 1 | -0.085299459 | 0.011174007 | -7.633739552 | **3.04209E-12** | -0.107388358 | -0.063210559 |

**Since p=3.04209E-12 (<0.05), linear correlation coefficient value is significant at 5% level.**

***6.2. Warming trends*- Example of regression graph**

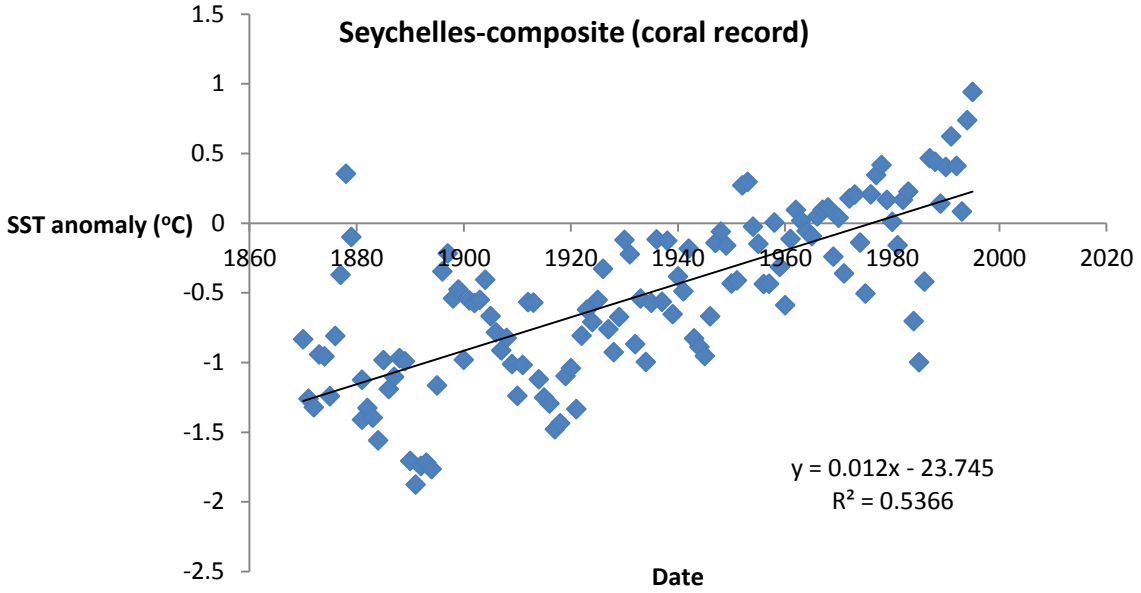


**Gradient=+0.012 °C/year**

**Period= 1870-1995 (126 years)**

**Warming trend (SST change) for period=+0.012*126=+1.51 °C**

**Figure 6.2. Graph showing the trend analysis of coral record for Seychelles-composite from 1870-1995**

**Table 6.2. Coefficients, Standard Error, t-stat, p-value, lower and upper limit of 95% C.I for regression in Figure 6.2.**

| | *Coefficients* | *Standard Error* | *t Stat* | *P-value* | *Lower 95.0%* | *Upper 95.0%* |
|---|---|---|---|---|---|---|
| Intercept | -23.74517069 | 1.938068817 | -12.251975 | 4.1978E-23 | -27.58115172 | -19.90918967 |
| X Variable 1 | 0.012015584 | 0.0010027 | 11.98322844 | **1.88289E-22** | 0.01003096 | 0.014000208 |

**Since p=1.88289E-22 (<0.05), the SST change is significant at the 5% level.**

### *6.3. Warming trends*- Test results

**Table 6.3. Test results for the Mann-Whitney U-Test performed on mean annual coral records, ERSSTv3 and HadSST1.1 data for 4 tropical and 7 tropical sites.**

| | Coral record | ERSSTv3 | HadSST1.1 |
|---|---|---|---|
| **Tropical** | +1.51 | +0.81 | +0.59 |
| | +0.41 | +0.61 | +0.47 |
| | +0.31 | +0.81 | +0.74 |
| | +1.05 | +0.69 | +0.66 |
| **Subtropical** | +0.96 | +0.34 | +0.53 |
| | +0.23 | +0.69 | +0.30 |
| | +0.28 | +0.35 | +0.12 |
| | +1.28 | +0.64 | +0.24 |
| | -0.49 | +0.07 | +0.50 |
| | +0.69 | +0.55 | +0.39 |
| | +0.80 | +0.39 | +0.40 |
| **Test results (Mann-Whitney U Test)** | U=9.0<br>p=0.395 (>0.05)<br>Not Significant at 5% level | **U=2.5**<br>**p=0.038 (<0.05)**<br>**Significant at 5% level** | **U=2.0**<br>**p=0.030 (<0.05)**<br>**Significant at 5% level** |

**Table 6.4. Test results for the Mann-Whitney U-Test performed on coral records, ERSSTv3 and HadSST1.1 data for 3 tropical and 7 tropical sites during summer period.**

| | Coral record | ERSSTv3 | HadSST1.1 |
|---|---|---|---|
| **Tropical** | +1.45 | +0.74 | +0.63 |
| | +0.56 | +0.60 | +0.39 |
| | +1.10 | +0.65 | +0.64 |
| **Subtropical** | +1.04 | +0.33 | +0.52 |
| | +0.09 | +0.51 | +0.19 |
| | +1.12 | +0.31 | +0.14 |
| | +1.14 | +0.50 | +0.16 |
| | -0.34 | +0.08 | +0.45 |
| | +0.59 | +0.45 | +0.26 |
| | +0.46 | +0.39 | +0.33 |
| **Test results (Mann-Whitney U Test)** | U=6.0<br>p=0.362 (>0.05)<br>Not Significant at 5% level | **U=0**<br>**p=0.023 (<0.05)**<br>**Significant at 5% level** | U=2.0<br>p=0.068 (<0.05)<br>Not Significant at 5% level |

**Table 6.5. Test results for the Mann-Whitney U-Test performed on coral records, ERSSTv3 and HadSST1.1 data for 3 tropical and 7 tropical sites during winter period.**

| | Coral record | ERSSTv3 | HadSST1.1 |
|---|---|---|---|
| Tropical | +1.55 | +0.88 | +0.53 |
| | +0.26 | +0.61 | +0.54 |
| | +1.03 | +0.73 | +0.68 |
| Subtropical | +0.87 | +0.34 | +0.52 |
| | +0.39 | +0.86 | +0.40 |
| | -0.62 | +0.39 | +0.10 |
| | +1.40 | +0.78 | +0.33 |
| | -0.63 | +0.07 | +0.54 |
| | +0.77 | +0.64 | +0.52 |
| | +1.14 | +0.38 | +0.47 |
| Test results (Mann-Whitney U Test) | U=7.0<br>p=0.494 (>0.05)<br>Not Significant at 5% level | U=5.0<br>p=0.254 (<0.05)<br>Not Significant at 5% level | U=1.5<br>p=0.052 (<0.05)<br>Not Significant at 5% level |

**Table 6.6. Test results for Lord's Range Test performed on coral records, ERSSTv3 and HadSST1.1 data respectively while comparing summer and winter trends for the tropical region.**

| Coral record | | ERSSTv3 | | HadSST1.1 | |
|---|---|---|---|---|---|
| **summer** | **winter** | **summer** | **winter** | **summer** | **winter** |
| +1.45 | +1.55 | +0.74 | +0.88 | +0.63 | +0.53 |
| +0.56 | +0.26 | +0.60 | +0.61 | +0.39 | +0.54 |
| +1.10 | +1.03 | +0.65 | +0.73 | +0.64 | +0.68 |
| Test results:<br><br>L=0.0413, L for p=5% =0.64<br><br>No Significant difference at 5% level | | Test results:<br><br>L=0.187, L for p=5% =0.64<br><br>No Significant difference at 5% level | | Test results:<br><br>L=0.0750, L for p=5% =0.64<br><br>No Significant difference at 5% level | |

**Table 6.7. Test results for the Wilcoxon Matched Paired Sample Test performed on coral records, ERSSTv3 and HadSST1.1 data respectively while comparing summer and winter trends for the subtropical region.**

| **Coral record** | | **ERSSTv3** | | **HadSST1.1** | |
|---|---|---|---|---|---|
| **summer** | **winter** | **summer** | **winter** | **summer** | **winter** |
| +1.04 | +0.87 | +0.33 | +0.34 | +0.52 | +0.52 |
| +0.09 | +0.39 | +0.51 | +0.86 | +0.19 | +0.40 |
| +1.12 | -0.62 | +0.31 | +0.39 | +0.14 | +0.10 |
| +1.14 | +1.40 | +0.50 | +0.78 | +0.16 | +0.33 |
| -0.34 | -0.63 | +0.08 | +0.07 | +0.45 | +0.54 |
| +0.59 | +0.77 | +0.45 | +0.64 | +0.26 | +0.52 |
| +0.46 | +1.14 | +0.39 | +0.38 | +0.33 | +0.47 |
| Test results:<br><br>T=12.0, p=0.735 (>0.05)<br><br>No Significant difference at 5% level | | Test results:<br><br>T=4.50, p=0.108 (>0.05)<br><br>No Significant difference at 5% level | | **Test results:**<br><br>**T=1.0, p=0.0464 (<0.05)**<br><br>**Significant difference at 5% level** | |

**Acknowledgements**

I would like to thank my supervisor Prof. Chris Reason and my co-supervisor Dr. Jens Zinke for their guidance, patience, precious advice and critical comments during the project. My sincere thanks also go to Mr. Gamoyo Majambo for assistance in data analysis. Furthermore, help and support from AMS 2011 and MA-RE colleagues are gratefully acknowledged.

**References**

Allan, R.J., Lindesay, J.A. & Reason, C.J.C. 1995. Multidecadal variability in the climate system over the Indian Ocean region during the austral summer. *Journal of Climate*, vol. 8, pp. 1853–1873.

Ashok, K., Guan, Z. & Yamagata, T. 2003. A look at the relationship between the ENSO and the Indian Ocean Dipole. *Journal of the Meteorological Society of Japan*, vol. 81, no. 1, pp. 41-56.

Ateweberhan, M. & McClanahan, T.R. 2010. Relationship between historical sea-surface temperature variability and climate change-induced coral mortality in the western Indian Ocean. *Marine Pollution Bulletin*, vol. 60, pp. 964–970.

Azman, J., Frković, V., Bilić-Zulle, L. & Petrovecki, M. 2006. Correlation and regression. *Circulation*, vol. 60, no. 19, pp. 2083-2088.

Beck, J.W., Edwards, R.L., Ito, E., Taylor, F.W., Recy, J., Rougerie, F., Joannot, P. & Henin, C. 1992. Sea-surface temperature from coral skeletal strontium/calcium ratios. *Science,* vol. 257, no. 5070, pp. 644.

Cai, W., Hendon, H.H. & Meyers, G. 2005. Indian Ocean Dipole like variability in the CSIRO mark 3 coupled climate model. *Journal of Climate*, vol. 18, pp. 1449–1468.

Carilli, J.E., Norris, R.D., Black, B., Walsh, S.M. & McField, M. 2010. Century-scale records of coral growth rates indicate that local stressors reduce coral thermal tolerance threshold. *Global Change Biology,* vol. 16, no. 4, pp. 1247.

Charles, C.D., Cobb, K., Moore, M.D. & Fairbanks, R.G. 2003. Monsoon–tropical ocean interaction in a network of coral records spanning the 20th century. *Marine Geology,* vol. 201, no. 1-3, pp. 207-222.

Charles, C.D., Hunter, D.E. & Fairbanks, R.G. 1997. Interaction between the ENSO and the Asian monsoon in a coral record of tropical climate. *Science,* vol. 277, no. 5328, pp. 925.

Cobb, K., Cole, J., Lough, J. & Tudhope, S. 2008. Annually-banded corals as climate proxies, *White Paper* for Trieste Meeting, 9-11 June.

Cole, J.E., Dunbar, R.B., McClanahan, T.R. & Muthiga, N.A. 2000. Tropical Pacific forcing of decadal SST variability in the western Indian Ocean over the past two centuries. *Science,* vol. 287, no. 5453, pp. 617-619.

Cole, J.E., Fairbanks, R.G. & Shen, G.T. 1993. Recent variability in the Southern Oscillation: isotopic results from a Tarawa Atoll coral. *Science,* vol. 260, no. 5115, pp. 1790-1793.

Corrège, T. 2006. Sea surface temperature and salinity reconstruction from coral geochemical tracers. *Palaeogeography, Palaeoclimatology, Palaeoecology,* vol. 232, no. 2-4, pp. 408.

Crueger, T., Zinke, J. & Pfeiffer, M. 2009. Patterns of Pacific decadal variability recorded by Indian ocean corals. *International Journal of Earth Sciences,* vol. 98, pp. 41-52.

Damassa, T.D., Cole, J.E., Barnett, H.R., Ault, T.R. & McClanahan, T.R. 2006. Enhanced multidecadal climate variability in the seventeenth century from coral isotope records in the western Indian Ocean. *Paleoceanography,* vol. 21, no. PA2016.

DeLong, K. L., Quinn, T.M., Shen, C.-C. & Lin, K. 2010. A snapshot of climate variability at Tahiti at 9.5 ka using a fossil coral from IODP Expedition 310. *Geochemistry Geophysics Geosystems*, vol. 11, Q06005.

Deser, C., Phillips, A.S. & Hurrell, J.W. 2004. Pacific interdecadal climate variability: linkages between the tropics, the North Pacific during boreal winter since 1900. *Journal of Climate,* vol. 17, no. 16, pp. 3109–3124.

Donner, S.D. 2011. An evaluation of the effect of recent temperature variability on the prediction of coral bleaching events. *Ecological Applications*, vol. 21, no. 5, pp. 1718–1730.

Eakin, C.M. & Grottoli, A.G. 2006. Coral reef records of past climatic change. In *Paleo-climate changes and corals. In: Coral Reefs and Climate Change: Science and Management*, eds. Phinney, J., Skirving, W., Kleypas, J., Hoegh-Guldberg, O. & Strong, A.E., Coastal and Estuarine Studies, pp. 33.

Gagan, M.K., Ayliffe, L.K., Hopley, D., Cali, J.A., Mortimer, G.E., Chappell, J., McCulloch, M.T. & Head, M.J. 1998. Temperature and surface-ocean water balance of the mid-Holocene tropical western Pacific. *Science,* vol. 279, no. 5353, pp. 1014.

Gagan, M.K., Ayliffe, L.K., Beck, J.W., Cole, J.E., Druffel, E.R.M., Dunbar, R.B. & Schrag, D.P. 2000. New views of tropical paleoclimates from corals. *Quaternary Science Reviews,* vol. 19, no. 1-5, pp. 45-64.

Gagan, M.K., Dunbar, G.B. & Suzuki, A. 2012. The effect of skeletal mass accumulation in *Porites* on coral Sr/Ca and d18O paleothermometry. *Paleoceanography*, vol. 27, PA1203.

Goreau, T.J. & Hayes, R.M. 1994. Coral bleaching and ocean "Hotspots". *Ambio*, vol. 23, pp. 176-180.

Hendy, E.J., Gagan, M.K., Alibert, C.A., McCulloch, M.T., Lough, J.M. & Isdale, P.J. 2002. Abrupt decrease in tropical Pacific sea surface salinity at end of Little Ice Age. *Science,* vol. 295, no. 5559, pp. 1511.

Hess, A., Iyer, H. & Malm, W. 2001. Linear trend analysis: a comparison of methods. *Atmospheric Environment*, vol. 35, pp. 5211-5222.

Hoegh-Guldberg, O. 1999. Climate change, coral bleaching and the future of the world's coral reefs. *Marine Freshwater Research,* vol. 50, pp. 839.

Hong, C.C., Lu, M.M. & Kanamitsu, M. 2008. Temporal and spatial characteristics of positive and negative Indian Ocean dipole with and without ENSO. *Journal of Geophysical Research*, vol. 113, D08107.

Jaisingh, L. 2005. Exploring bivariate data. In *Statistics for the utterly confused*, 2nd edition, eds. Gilson, B. and Walker, M., McGraw-Hill, United States, pp. 82-94.

Juillet-Leclerc, A., Jouzel, J., Labeyrie, L. & Joussaume, S. 1997. Modern and last glacial maximum sea surface δ18O derived from an Atmospheric General Circulation Model. *Earth and Planetary Science Letters,* vol. 146, no. 3-4, pp. 591-605.

Juillet-Leclerc, A., & Schmidt, G. 2001. A calibration of the oxygen isotope paleothermometer of coral aragonite from *Porites*. *Geophysical Research Letters*, vol. 28, no. 21, pp. 4135-4138.

Kim, S. & O'Neil, J.R. 1997. Equilibrium and nonequilibrium oxygen isotope effects in synthetic carbonates. *Geochimica et Cosmochimica Acta,* vol. 61, no. 16, pp. 3461-3475.

Linsley, B.K., Rosenthal, Y. & Oppo, D.W. 2010. Holocene evolution of the Indonesian throughflow and the western Pacific warm pool. *Nature Geoscience*, vol. 3, pp. 578–583.

Linsley, B.K., Wellington, G.M., Schrag, D.P., Ren, L., Salinger, M.J. & Tudhope, A.W. 2004. Geochemical evidence from corals for changes in the amplitude and spatial pattern of South Pacific interdecadal climate variability over the last 300 years. *Climate Dynamics*, vol. 22, pp. 1–11.

Lough, J.M. 2000. 1997-98: Unprecedented thermal stress to coral reefs? *Geophysical Research Letters,* vol. 27, no. 23, pp. 3901.

Lough, J.M. 2010. Climate records from corals. *Wiley Interdisciplinary Reviews: Climate Change,* vol. 1, no. 3, pp. 318-331.

MacMynowski, D.G. & Tziperman, E. 2008. Factors affecting ENSO's period. *Journal of the Atmospheric Sciences*, vol. 65, pp. 1570-1585.

Mantua, N.J. & Hare, S.R. 2002. The Pacific Decadal Oscillation. *Journal of Oceanography*, vol. 58, pp. 35-44.

McCarthy, J.J., Canziani, O.F., Leary, N.A., Dokken, D.J. & White, K.S. 2001. Climate Change 2001: impacts, adaptation, and vulnerability. Contribution of Working Group II to the third assessment report of the Intergovernmental Panel on Climate Change (IPCC). Cambridge University Press, Cambridge, UK.

McClanahan, T.R., Ateweberhan, M., Muhando, C.A., Maina, J. & Mohammed, M.S. 2007. Effects of climate and seawater temperature variation on coral bleaching and mortality. *Ecological Monographs,* vol. 77, no. 4, pp. 503.

McClanahan, T.R., Ateweberhan, M., Omukoto, J. & Pearson, L. 2009. Recent seawater temperature histories, status, and predictions for Madagascar's coral reefs. *Marine Ecology Progress Series*, vol. 380, pp. 117–128.

McClanahan, T.R., Maina, J.M. & Muthiga, N.A. 2011. Associations between climate stress and coral reef diversity in the western Indian Ocean. *Global Change Biology,* vol. 17, pp. 2023.

Meyers, G.A., McIntosh, P.C., Pigot, L. & Pook, M.J. 2007. The years of El Niño, La Niña and interactions with the tropical Indian Ocean. *Journal of Climate,* vol. 20, pp. 2872-2880.

National Climatic Data Centre. 2009. Significant Historical ENSO Events. Available online at: http://ncdc.noaa.gov/teleconnections/enso/enso-sigevents.php. (Last accessed 23rd June 2012).

Obura, D.O. 2005. Resilience and climate change: lessons from coral reefs and bleaching in western Indian Ocean. *Estuarine Coastal and Shelf Science,* no. 63, pp. 353-372.

Pfeiffer, M. & Dullo, W. 2006. Monsoon-induced cooling of the western equatorial Indian Ocean as recorded in coral oxygen isotope records from the Seychelles covering the period of 1840–1994 AD. *Quaternary Science Reviews,* vol. 25, no. 9-10, pp. 993-1009.

Pfeiffer, M., Dullo, W. & Eisenhauer, A. 2004a. Variability of the Intertropical Convergence Zone recorded in coral isotopic records from the central Indian Ocean (Chagos Archipelago). *Quaternary Research,* vol. 61, no. 3, pp. 245-255.

Pfeiffer, M., Timm, O., Dullo, W. & Podlech, S. 2004b. Oceanic forcing of interannual and multidecadal climate variability in the south western Indian Ocean: Evidence from a 160 year coral isotopic record (La Réunion, 55°E, 21°S). *Paleoceanography,* vol. 19, no. PA4006.

Rayner, N.A., Parker, D.E., Horton, E.B., Folland, C.K., Alexander, L.V., Rowell, D.P., Kent, E.C. & Kaplan, A. 2003. Global analyses of sea surface temperature, sea ice, and night marine air temperature since the late nineteenth century. *Journal of Geophysical Research*, no. 108, pp. 4407.

Reason, C., Allan, J., Lindesay, J. & Ansell, T. 2000. ENSO and climatic signals across the Indian Ocean basin in the global context: Part I, interannual composite patterns. *International Journal of Climatology*, vol. 20, pp. 1285–1327.

Reason, C.J.C. & Rouault, M. 2002. ENSO-like decadal variability and South African rainfall. *Geophysical Research Letters,* vol. 29, no.13, pp. 1638-1641.

Reynolds, R.W., Smith, T.M., Liu, C., Chelton, D.B., Casey, K.S. & Schlax, M.G. 2007. Daily high-resolution-blended analyses for sea surface temperature. *Journal of Climate,* vol. 20, pp. 5473-5496.

Saji, N.H., Goswami, B.N., Vinayachandran, P.N. & Yamagata, T. 1999. A dipole mode in the tropical Indian Ocean. *Nature*, vol. 401, pp. 360-363.

Scott, R.B., Holland, C.L. & Quinn, T.M. 2010. Multidecadal trends in instrumental SST and coral proxy Sr/Ca records. *Journal of Climate,* vol. 23, no. 5, pp. 1017.

Sheppard, C.R.C. 2003. Predicted recurrences of mass coral mortality in the Indian Ocean. *Nature,* vol. 425, pp. 294-297.

Smith, T.M. & Reynolds, R.W. 2003. Extended reconstruction of global sea surface temperatures based on COADS data (1854-1997). *Journal of Climate,* vol. 16, no. 10, pp. 1495.

Smith, T.M., Reynolds, R.W., Peterson, T.C. & Lawrimore, J. 2008a. Improvements to NOAA's historical merged land-ocean surface temperature analysis (1880-2006). *Journal of Climate,* vol. 21, no. 10, pp. 2283.

Smith, L., Gilmour, J.P. & Heyward, A.J. 2008b. Resilience of coral communities on an isolated system of reefs following catastrophic mass-bleaching. *Coral Reefs*, no. 27, pp. 197–205.

Spalding, M., Ravilious, C. & Green, E.P. 2001. World Atlas of Coral Reefs. In *UNEP World Conservation Monitoring Centre*, University of California Press, Berkeley, USA, pp. 180.

Strong, A.E., Barrientos, C.S., Duda, C. & Saper, J. 1997. Improved satellite techniques for monitoring coral reef bleaching. *Proceedings of the 8th International Coral Reef Symposium*, eds. Lessios, H.A, & Macintyre, I.G., Mithsonian Tropical Research Institute, Panama, pp. 1495.

Torrence, C. & Compo, G. P. 1998. A practical guide to wavelet analysis. *Bulletin of the American Meteorological Society*, vol. 79, no. 1, pp. 61–78.

Ummenhofer, C.C., England, M.H., McIntosh, P.C., Meyers, G.A., Pook, M.J., Risbey, J.S., Sen Gupta, A. & Taschetto, A.S. 2009. What causes southeast Australia's worst droughts? *Geophysical Research Letters,* vol. 36, no. L04706

West, J.M. & Salm, R.V. 2003. Resistance and resilience to coral bleaching: implications for coral reef conservation and management. *Conservation Biology,* vol. 17, pp. 956–967.

Wilkinson, C. 2000. Status of Coral Reefs of the World: 2000. Australian Institute of Marine Science, Townsville.

Zinke, J., Dullo, W., Heiss, G.A. & Eisenhauer, A. 2004b. ENSO and Indian Ocean subtropical dipole variability is recorded in a coral record off southwest Madagascar for the period 1659 to 1995. *Earth and Planetary Science Letters,* vol. 228, no. 1-2, pp. 177.

Zinke, J., Pfeiffer, M., Timm, O., Dullo, W. & Brummer, G.J.A. 2009. Western Indian Ocean marine and terrestrial records of climate variability: a review and new concepts on land–ocean interactions since AD 1660. *International Journal of Earth Sciences,* vol. 98, no. 1, pp. 115.

Zinke, J., Pfeiffer, M., Timm, O., Dullo, W. & Davies, G.R. 2005. Atmosphere-ocean dynamics in the western Indian Ocean recorded in corals. *Philosophical Transactions: Mathematical, Physical and Engineering Sciences,* vol. 363, no. 1826, pp. 121-142.

Zinke, J., Pfeiffer, M., Timm, O., Dullo, W., Kroon, D. & Thomassin, B.A. 2008. "Mayotte coral reveals hydrological changes in the western Indian Ocean between 1881 and 1994". *Geophysical Research Letters,* vol. 35, no. 23, pp. L23707.

Zinke, J., Von Storch, H., Mueller, B., Zorita, E., Rein, B., Mieding, B.A. & KIHZ- Consortium *et al.* 2004a. Evidence for the climate during the Late Maunder Minimum from proxy data and model simulations available within KIHZ. In *The climate in historical times— towards a synthesis of Holocene proxy data and climate models*, eds. von Storch, H., Raschke, E. & Floeser, G., Springer, Berlin.